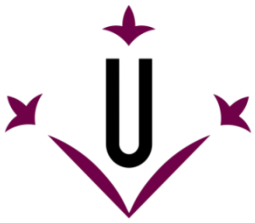

Citation: Piqué, G., Batalla, R.J., López, R., Sabater, S., 2017. The fluvial sediment budget of a dammed river (upper Muga, southern Pyrenees). *Geomorphology* 293, 211–226. http://dx.doi.org/10.1016/j.geomorph.2017.05.018.

The fluvial sediment budget of a dammed river (upper Muga, southern Pyrenees)

Piqué, G.[1,2,*], **Batalla, R.J.**[1,2,3], **López, R.**[2], **Sabater, S.**[1,4]

[1] Catalan Institute for Water Research, H_2O Building, E-17003, Girona, Catalonia, Spain

[2] RIUS, Fluvial Dynamics Research Group, University of Lleida, Lleida, Catalonia, Spain

[3] Faculty of Forest Sciences and Natural Resources, Austral University of Chile, Valdivia, Chile

[4] GRECO, Institute of Aquatic Ecology, University of Girona, Girona, Catalonia, Spain

[*]Corresponding author. E-mail: gpiquealtes@gmail.com.

Abstract

Many rivers in the Mediterranean region are regulated for urban and agricultural purposes. Reservoir presence and operation results in flow alteration and sediment discontinuity, altering the longitudinal structure of the fluvial system. This study presents a 3-year sediment budget of a highly dammed Mediterranean river (the Muga, southern Pyrenees), which has experienced flow regulation since the 1969 owing to a 61-hm^3 reservoir. Flow discharge and suspended sediment concentration were monitored immediately upstream and downstream from the reservoir, whereas bedload transport was estimated by means of bedload formulae and estimated from regional data. Results show how the dam modifies river flow, reducing the magnitude of floods and shortening its duration. At the same time, duration of low flows increases. The downstream flow regime follows reservoir releases that are mostly driven by the irrigation needs in the lowlands. Likewise, suspended sediment and bedload transport are shown to be notably affected by the dam. Sediment transport upstream was mainly associated with floods and was therefore concentrated in short periods of time (i.e., > 90% of the sediment load occurs in < 1% of the time). Downstream from the dam, sediments were transported more constantly (i.e., 90% of the load was carried during 50% of the time). Total sediment load upstream from the dam equalled 23,074 t, while downstream it was < 1000 t. Upstream, sediment load was equally distributed between suspension and bedload (i.e., 10,278 and 12,796 t respectively), whereas suspension dominated sediment transport downstream. More than 95% of the

sediments transported from the upstream basins were trapped in the reservoir, a fact that explains the sediment deficit and the river bed armouring observed downstream. Overall, the dam disrupted the natural water and sediment fluxes, generating a highly modified environment downstream. Below the dam, the whole ecosystem shifted to stable conditions owing to the reduction of water and sediment loads.

Keywords: sediment budget; suspended sediment; bedload; dams; Mediterranean basin; River Muga

1. Introduction

A sediment budget describes and quantifies the spatial and temporal distribution of sediment produced, eroded, stored, and transferred within a drainage basin and, ultimately, exported out of it (Dietrich and Dunne, 1978; Dietrich et al., 1982; Slaymaker, 2003). Rivers and their sediment loads are central components of basins' sediment budgets and provide useful information of the effects of human interventions in the catchment, such as reservoir siltation and the consequent sediment deficit below dams, instream gravel mining, and river training among others (e.g., Kondolf, 1997; Vericat and Batalla, 2006). Sediment budgets have also proven to be fundamental for interpreting biophysical processes in river channels, e.g., fish habitat suitability, river bed structure and clogging, and invertebrate drift and vegetative succession (e.g., Trimble, 2004; Merz et al., 2006; Buendia et al., 2014). The amount of sediment generated in a basin, and subsequently transported through the drainage network, depends on the catchment area, climate, lithology, land uses, and in general, related human activities (e.g., Kesel et al., 1992). Overall, atmospheric factors play a central role in controlling runoff generation and soil erosion and are the main cause of the intra-annual variability in sediment yields (Nadal-Romero et al., 2015). In particular, and from a worldwide perspective, erosive processes are relatively more intense in Mediterranean basins, as has been reported extensively (e.g., Inbar, 1992; Walling and Webb, 1996; Gallart et al., 2005; Lopez Saez et al., 2011; López-Tarazón et al., 2011; Vanmaercke et al., 2011; García-Ruiz et al., 2013; Vachtman

et al., 2013), while most of the sediment is generally transported during a few events (i.e., time-compression of erosion processes is acute; e.g., Gonzalez-Hidalgo et al., 2007, 2013).

Sediment budgets have mainly focused on the particulate sediments that are transported in suspension (Richards, 1982), but dissolved loads and bedloads may also represent an important proportion of the total sediment load. The dissolved load in a river is the product of inputs from rainfall and dry deposition (Meybeck, 1983), rock and soil weathering (Drever, 1982), and biogeochemical processes derived from natural processes and human activities (Farley and Werritty, 1989). Dissolved load dominates the denudation processes in forested areas of humid climates (Sala and Wheeler, 1988; Farley and Werritty, 1989). Bedload is usually a small part of the total load (around 10%, on average), but values range from below 1% in lowland rivers to up to 70% in mountain streams (Richards, 1982). Transport of fine sediments occurs in relation to erosional processes in the upstream basin and is referred to as *wash-load*, typically transported in suspension almost continuously (concentrations may be high even in some low flows; e.g., López-Tarazón et al., 2011).

Suspended sediment transport was typically measured by means of direct sampling until the 1980s, when continuous records could be obtained through optical turbidity sensors (Downing, 2006). The main advantage of continuous measurements is that they allow improved estimations of sediment loads, in comparison to the statistical procedures that must be used when only discrete samples are available. However, turbidity records require individual and *in situ* calibration, as several factors affect sensor readings (Downing, 2006; Minella, et al., 2008; Merten et al., 2013; Regüés and Nadal-Romero, 2013). Unlike suspended sediment, bedload transport is not continuous and generally occurs only during floods. The measurement of bedload has numerous technical difficulties (Hubbell et al., 1987), and bedload data are sparse and discontinuous. In light of these practical shortcomings, a number of equations have been developed, most of them derived from flume experimental data (e.g., Brown, 1950; Hamamori, 1962; Wong and Parker, 2006); whereas others also considered field observations (Gomez and Church, 1989). Numerous equations focus on the bedload discharge prediction in gravel-bedded

rivers in which the role of armour layers and the grain size distribution of sediment mixtures need to be carefully determined prior to model application (e.g., Bathurst, 2007). Several works have been undertaken to test the predictive power of bedload equations and its applicability to the estimation of rivers' load (e.g., White et al., 1975; Batalla, 1997; Habersack and Laronne, 2002; Barry et al., 2008; López et al., 2014, 2015).

Fluvial sediment budgets have been developed at different scales, ranging from the catchment (e.g., Loughran, 1992; Batalla et al., 1995; Lobera et al., 2016), to regional (e.g., Vanmaercke et al., 2011; Buendia et al., 2016), and continental/planetary (e.g., Walling, 2008) scales. In Europe, dissolved load dominates in rivers of temperate regions, while European Mediterranean rivers are controlled by suspended loads, owing to the more intense erosion processes in the basin (Milliman, 2001). There, rainfall episodes are often short but intense, triggering soil detachment and transport in sparsely vegetated areas. Further, water scarcity in this region has historically triggered the building of reservoirs for agricultural and urban purposes, so most rivers in the western Mediterranean are dammed (Beaumont, 1978). One of the main effects of dams is the reduction of flood magnitude and frequency (e.g., in California, Kondolf and Batalla, 2005; in the Mediterranean, Batalla et al., 2004; Piqué et al., 2016), and consequently, the sediment budget of the dammed river becomes altered (e.g., Williams and Wolman, 1984; Vericat and Batalla, 2006). Typically, the large part of the sediment transported through the fluvial network is retained in the reservoir and the sediment transfer is interrupted downstream, particularly the bedload, which is completely trapped. In addition, the lack of river bed disturbance in reaches downstream from dams progressively leads to stabilisation (e.g., Vericat et al., 2006; Draut et al., 2011; Lobera et al., 2016). The reduction of hydrologically active areas and substratum heterogeneity and complexity has implications for the ecosystem functioning, as energy fluxes change, potential habitat is reduced (Graf, 2006; Batalla and Vericat, 2013) and water quality is altered (Goodwin et al., 2006).

A greater understanding of the effects of global change on river basins requires further efforts to quantify flow and sediment fluxes through drainage networks. Working hypotheses are that the

water and sediment budgets are highly altered by the presence of dams and that these changes generate a reduction of delivered sediments and alter the overall downstream sedimentary dynamics. Within this context, studies focusing on basins in Mediterranean regions are still scarce and, to address this shortcoming, we constructed the sediment budget of a highly regulated river, the upper River Muga (southern Pyrenees, NE Iberian Peninsula, NW Mediterranean Sea). Among the NW mesoscale Mediterranean catchments that flow directly into the sea, the Muga is one of the most altered owing to dam presence in terms of hydrology (Piqué et al., 2016). In addition to the dam, the river is affected by changes in climate and other anthropic pressures (i.e., rising water demands), making it representative of the hydrosedimentary dynamics of rivers in the region. We therefore considered to (i) construct the sediment budget of a highly regulated Mediterranean river; (ii) determine the role of the reservoir on the upper basin water and sediment dynamics; and (iii) quantify the sediment deficit downstream from the dam. In order to achieve these objectives, the study has considered obtaining the water yield and the sediment transport of the two main subcatchments draining into the reservoir and has also considered the water and sediment released from the dam. Besides flow discharge, this paper quantifies the suspended sediment transport as well as the bedload, in order to achieve a more complete evaluation of the sediment fluxes. The findings provide a detailed view of the structural physical changes that affect river dynamics below dams, producing valuable information potentially applicable for management plans in highly modified fluvial environments.

2. Study area

The River Muga is located in the NE of the Iberian Peninsula. It drains an area of 758 km^2 of the southeasternmost section of the Pyrenean and the Albera ranges (Fig. 1). The altitude of the basin varies from 1443 m asl at Montnegre (NW) to sea level at the Gulf of Roses in the Mediterranean Sea (SE). The basin belongs to the Mediterranean climate domain and displays a notable variation in temperature and precipitation. Mean annual temperature in the Empordà depression (i.e., centre of the basin) is 14.5ºC, whereas in the headwaters it varies from 11ºC to

13ºC. Mean annual precipitation shows a W-E gradient ranging from > 1100 mm in the headwaters to 600 mm at the river mouth. The river flow is regulated by the Darnius-Boadella Dam, a 61 hm^3 (i.e., 1 $hm^3 = 1\times10^6$ m^3) impoundment built in 1969 to ensure water supply mostly for agricultural and urban uses in the lowlands but also to produce hydropower and for flood control. The dam was constructed at the confluence of the mainstem River Muga and its tributary Arnera (Fig. 1). For the purpose of this study, the analysis has been restricted to the upper part of the catchment (upper Muga), which includes (i) the Arnera, (ii) the Rimal, (iii) the Muga upstream from the dam (hereafter $Muga_{up}$) subbasins, and (iv) part of the basin downstream from the dam. However, the Rimal was not monitored, and therefore it is not included in the sediment budget. This tributary had a minor role in the hydrosedimentary dynamics of the basin, as the Arnera and the $Muga_{up}$ subbasins together comprise 90% of the upstream basin area. The terminology we use in the paper refers to the subbasin or to the specific sampling sites; as such, the sampling site for the Arnera subbasin is EA051, the site for the $Muga_{up}$ subbasin is EA050, and the sampling point downstream the dam is EA012 (see Fig. 1 for the exact location of these sites).

The Arnera is 60.5 km^2 and is lying on Palaeozoic granites and marls, while the $Muga_{up}$ is 84.1 km^2 and overlies Paleogene and Cretaceous marls and conglomerates. Forest constitutes the main land cover in both subbasins, occupying > 90% of the area and increasing up to 95% if scrubland is included. The impoundment runoff ratio of the reservoir (IR, as per Batalla et al., 2004) is 0.99 (Piqué et al., 2016), indicating that the reservoir regulates virtually all of the upper Muga basin's annual runoff. The river bed material in the mainstem Muga (upstream and downstream from the reservoir) is composed by a mixture of sands and gravels, with a well-developed armour layer in both cases. Channel slope is 0.80% and 0.84% respectively. The median size of surface river bed material (D_{50}) upstream from the dam (EA050 site) is 75.0 mm for the surface and 37.4 mm for the subsurface material, while D_{84} equalled 127.1 and 72.8 mm respectively. The armouring ratio is 2, which indicates that the river bed is armoured. Downstream the dam, median surface particle size is 54.9 mm, and subsurface material is 13.84

mm. The D_{84} is 123.1 and 44.4 mm for surface and subsurface material respectively. The armouring ratio is 4, indicating strong armouring. The downstream reach of the Arnera flows on bedrock and sands, with a mean channel slope of 0.85%. River bed is mainly composed of sands and bedrock, with a D_{50} particle size of 1.0 mm and D_{84} of 6.4 mm.

The basin has a rainfed hydrological regime, with marked seasonality. Mean monthly flows before dam construction showed two peaks (in spring and autumn) and a minimum in summer, reflecting the Mediterranean nature of the river; while after dam construction they are inversed and maximum discharges are released in summer to satisfy water demands for agriculture and tourism (Piqué et al., 2016). The mean flow discharge prior to construction of the dam was 2.34 $m^3 s^{-1}$ (SD = 1.29 $m^3 s^{-1}$, 1912-1969, n = 46 years), resulting in an average annual water yield of 73.8 hm^3. After damming, mean annual flow discharge is 1.98 $m^3 s^{-1}$ (SD = 1.13 $m^3 s^{-1}$, 1970-2011, n = 32 years), and the average annual water yield reduced to 62.6 hm^3. Such a 15% reduction can be related hypothetically to the combined effect of the evaporation losses from the reservoir and from the flow derived directly from the dam to attend urban demands of the Figueres urban area (Fig. 1). However, no reliable information is available to quantify the particular role of each of these factors on the observed runoff reduction after dam closure. Notably, the 1960s was by far the wettest decade during the twentieth century, a fact that could influence the computed mean for the pre-dam period. Magnitude and frequency of floods was notably affected by dam construction (see Piqué et al., 2016, for a flood frequency analysis on this river). For instance, the maximum daily flow reduced from 215 $m^3 s^{-1}$ for the pre-dam period to 193 $m^3 s^{-1}$ for the post-dam period). Owing to the Mediterranean character of the river, runoff varies notably between years: maximum water yield was 197.5 hm^3 in 1962-1963, whereas the minimum was recorded in 1998-1999 at 13.7 hm^3.

3. Data acquisition and analysis

3.1. Flow discharge

187 Flow stage (hereafter *h*) was recorded at 15-minute intervals for the 2012-2015 period with
188 sensors installed *ad hoc* at three gauging stations of the Catalan Water Agency (ACA; Fig. 1).
189 At EA050 ($Muga_{up}$) and EA051 (Arnera), *h* was measured by means of capacitive water stage
190 sensors (TruTrack® WT-HR, Intech Instruments LTD, Christchurch, New Zealand), while at
191 EA012 (downstream from the dam), a pair of pressure sensors (levelogger and barologger,
192 Solinst®, Georgetown, Canada) were used. Levelogger *h* data were corrected with
193 simultaneously recorded barologger air pressure measurements. Sensors were calibrated by
194 means of field observations, with regressions of $R^2 > 0.95$ in all cases. Corrected *h* data were
195 then transformed into flow discharge (hereafter *Q*) by means of the corresponding *h/Q* ACA
196 rating curves. An additional probe was installed downstream from EA050, where bed-material
197 movement was monitored. Here, several methods were used to derive and compare the *h*/*Q*
198 relation (i.e., slope-area method and statistically derived flow resistance equations developed by
199 López et al., 2007). As dispersion of the modelled curves was high, averaged results were used.
200 For consistency, *Q* was checked with values recorded at EA051. Furthermore, in EA012 (Fig.
201 1), hydrographs were routed upstream (reverse flow routing) until the section where bed-
202 material mobility was estimated, following the Muskingum method (Shaw, 1983). Finally, data
203 gaps in EA050 and EA051 were filled by relating the daily data of the two stations with the
204 relationship between Q_{EA050} and Q_{EA051} ($R^2 = 0.57$), which was then applied to complete the data
205 series. For consistency, results were cross-checked between the stations and against the volume
206 of water entering the reservoir.

207 *3.2. Suspended sediment*

208 Water turbidity (as a proxy of suspended sediment concentration, hereafter *SSC*) was recorded
209 at stations EA050, EA051, and EA012. Measurements were performed at 15-minute intervals
210 (averaged from 1-minute readings) for the 2012-2015 period, using Campbell® Optical
211 Backscatter Sensors OBS3+ and recorded in Campbell CR200x® dataloggers. The length of the
212 turbidity records varied between monitoring sites. Turbidity sensors (i.e., turbidimeters) were
213 calibrated by means of suspended sediment concentrations obtained from direct manual and

214 automatic water samples. Manual samples were taken fortnightly during low flows and
215 intensively during floods. Automatic samples were collected during floods at EA050 and
216 EA051 using respectively an ISCO 3700 (Teledyne Isco®, Lincoln, Nebraska, USA) and a
217 SIGMA SD900 (HACH®, Loveland, Colorado, USA) automatic sampler. A total of 148 samples
218 were used for the turbidity probe calibration at EA050, 31 samples at EA050, and 214 samples
219 at EA012. Samples were later filtered through Whatman GF/C glass microfiber filters (pore size
220 = 1.2 μm) or decanted when *SSC* was high. Samples were dried and the organic matter was
221 combusted to obtain the particulate *SSC*. Regressions between turbidity values and measured
222 *SSC* (Table 1) were applied to obtain continuous suspended sediment records (i.e., sedigraphs).
223 Calibration at site EA012 was performed using the complete *SSC* data set of the two upstream
224 stations because of the lack of suspended sediment data during high flows.

225 Statistically significant hourly *Q*-*SSC* linear relations (p-value < 0.001; Table 1, Fig. 2) were
226 obtained for EA050 and EA051 for the periods with available turbidity data, and these relations
227 were then used to extend the sedigraphs for the three hydrological years. Although *Q*-*SSC* rating
228 curves usually follow a power-law relationship (Syvitski et al., 2000), linear relationships
229 showed better results in the case of the Muga. Data distribution in EA050 and EA051 sites
230 indicate sediment supply limitation (more pronounced in EA051). In order to avoid a large
231 overestimation of the load in this site, two different linear relationships were used. In the case of
232 EA012, *Q* and *SSC* did not show a statistically significant relationship, and the six months of
233 missing data had to be derived from the monthly runoff-suspended sediment load relationship
234 (i.e., *WY*-*SSL*). This relationship was obtained from the data of the study period (i.e., October
235 2012-April 2015, n = 30) and was applied to runoff data at a monthly scale. The obtained linear
236 regression has an R^2 = 0.89 and a p-value < 0.01.

237 The described *Q*-*SSC* temporal extrapolations inevitably resulted in some uncertainties.
238 Although the correlations between *Q* and *SSC* reached an acceptable explanatory power and
239 were statistically significant, data scatter and regression errors were high (see Table 1 and Fig. 2
240 for details). This is evidence of the high variability of the sediment transport processes and the

241 difficulty of suspended load estimation (Smart et al., 1999). In fact, the use of *Q-SSC* rating
242 curves tends to underestimate loads (De Girolamo et al., 2015).

243 *3.3. Bed material and particle mobility*

244 *3.3.1. Grain-size distribution (GSD)*

245 Surface bed material in sites EA050 and EA012 was sampled twice (early 2013-2014 and early
246 2014-2015) in exposed bars following the pebble count method (Wolman, 1954). A total of 862
247 particles were measured in EA050, whereas 435 were surveyed in EA012. Subsurface materials
248 were characterised through volumetric sampling: three samples were taken in EA050 and two in
249 EA012, after the removal of the coarse surface layer (Church et al., 1987). In the EA051 river
250 reach and because of the particular characteristics of the river bed sediments (sand), three bulk
251 samples were collected. The volumetric samples were partly sieved in the field (i.e., the larger
252 size fractions), while the finest fractions were dried and sieved in the laboratory using a Filtra®
253 FLT-0200 electromagnetic sieve shaker (Filtra Vibración, Badalona, Spain).

254 *3.3.2. Cross-sectional geometry and flow hydraulics*

255 Cross-sectional topographic surveys were performed to characterise the channel geometry of the
256 three study sites. Cross sections were measured using a GPS (Leica® VIVA GS15) and a total
257 station (TPS, Leica® TS02), depending on the vegetation cover (GPS was used when vegetation
258 did not cover the river channel, i.e., in EA050; and TPS was used when vegetation was dense
259 and thus GPS signal was weak, i.e., in EA012 and EA051). From the cross sections and the *h/Q*
260 rating curves, the hydraulic parameters needed to apply the bedload equations were derived.
261 Hydraulic radius (R_h) and active channel width (w_a) were calculated for each value of Q. The
262 active channel width designates the fraction of the river bed where bedload transport occurs
263 (e.g., Tanguy, 2013) and is typically narrower than the bankfull channel (U.S. Geological
264 Survey, 2002) and the wetted width (Church et al., 2012). According to this, the maximum
265 active width was determined following two different methods related to bankfull Q: (i) the
266 breakpoint in the slope of the cross-sectional depth-width relation, and (ii) the limit of the

perennial vegetation. From the obtained values, the most restrictive one was used. Hence, the active channel width for the bedload calculations was defined as the top width for every *h* increment to a point from which it was established as a constant value, and *h* increments did not imply an increase in the active width. Channel slope (*S*) was used as a proxy of energy slope. Channel slope was measured for a distance of 20 times the bankfull width in EA051 and EA012 (e.g., Leopold and Skibitzke, 1967; Harrelson et al., 1994) and ca. 10 times at EA050, as weirs prevented enlarging the surveyed area.

3.3.3. Bedload formulae

Bedload transport was estimated from different formulae for the 2012-2015 period. In EA050 and EA012 (i.e., gravel beds) bedload was calculated applying the bedload formulae developed by Bathurst (2007) and Recking (2010). These equations predict the breakup or disruption of armour layer (if present) and are thus applicable to armoured gravel-bed rivers (e.g., for application of both formulae see López et al., 2015). The Bathurst (2007) formula predicts bedload Q in conditions of a broken armour layer; thus we assumed that in conditions of unbroken armour layer, bedload was negligible. The formula of Recking (2010) is a nonthreshold equation, though it predicts only very low values during low flows if the armour layer is unbroken. This formula allows for the differentiation of three phases of bedload transport, depending on the degree of particle mobility. With the aim of being conservative, the mean of the loads predicted by the two formulae was used for final sediment budget computations.

In EA051, we applied specific bedload equations for sandy gravel-bed rivers without an armour layer (Wong and Parker, 2006; Recking et al., 2013). The predicted values were very high (i.e., up to 80.5 kg s^{-1} m^{-1} for the Recking, 2013, equation), above reasonable bedload ranges reported in sandy rivers. For instance, Billi (2011) measured values < 1 kg s^{-1} m^{-1} for an ephemeral stream of slope = 1.3-1.4%; and Lucía et al. (2013) reported values up to 20 kg s^{-1} m^{-1} for a sandy stream of slope < 6%). We therefore based the estimation of bedload on previously

obtained results in nearby sand-bed rivers. We used data from the River Tordera (Rovira et al., 2005a and b) and applied a statistically significant relation between runoff and specific bedload transport ($R^2 = 0.64$). Although uncertainty is high given the variability of bedload transport, the R^2 value is sufficiently good to estimate bedload in the Arnera subbasin.

3.3.4. River bed mobility

In order to validate the results from bedload formulae (described in section 3.3.3), bed material mobility was monitored in the EA050 and EA012 river reaches from October 2013 to April 2015. We used flood episodes for which particle mobility was observed (i.e., competent flows) to allow for a qualitative comparison with equation predictions. Hence, we checked that mobility predicted by the equations actually corresponded to episodes when the armour layer broke up and the tracers mobilised.

In EA050 we used painted areas, RFID tagged tracers, and scour chains to detect mobility. Painted areas and radiofrequency tracers supply complementary information on particle displacement during competent floods, i.e., painted areas maintain the existing structure of the bar surface, while RFIDs can be placed within the wetted perimeter of the channel also allowing for the recovery of buried particles. Two 1×1 m areas were painted in the upstream part of the bar at both sites. Garish colour sprays were used to facilitate particle identification and recovery after flood disturbance. A total of 50 RFID tagged particles were also placed in two lines close to the painted areas. The particle size distribution of the RFID tracers was determined according to the surface GSD of the river reach (i.e., *b* axis ranged between 45 and 128 mm). After a competent flood, painted particles were visually identified and positioned with a GPS and/or a Total Station. The RFID tagged particles were identified using a pole antenna and an HDX Backpack Reader (Oregon RFID®, Portland, Oregon, USA) and also geopositioned. Tracers that moved < 1 m were not considered in order to minimize errors from the tag read range of the antenna. Moreover, four scour chains were installed in the head of the study bar to estimate the thickness of the active layer after each flood. The comparison between the length of visible

chain before and after a flood, as well as its position, gave information about the sequence of erosion and aggradation processes that occurred during a flood (Hassan, 1990; Nawa and Frissell, 1993; Powell et al., 2003). Finally, we assessed the movement of surface particles in EA012 by means of two painted areas that were periodically surveyed.

4. Results and discussion

4.1. Flow and sediment load upstream from the dam

4.1.1. Hydrology and runoff

The study period was drier than the long-term average: mean annual runoff 40.8 hm^3 for 2012-2015 *vs*. 73.8 hm^3 pre-dam data (i.e., 1912-1969) and 69.2 hm^3 of the complete data series (i.e., 1912-2011). Within the study period, the year 2013-2014 was the driest, with runoff being one-third of the mean value (Table 2); the year 2012-2013 was the wettest, but it still performed below the long-term average. The $Muga_{up}$ subbasin yielded more water than the Arnera because of its larger drainage area. Also the annual runoff coefficient (α) was higher at EA050 (0.25) than at EA051 (0.21). Mean Q entering the reservoir was 1.3 $m^3 s^{-1}$ for the 2012-2015 period (0.94 $m^3 s^{-1}$ from $Muga_{up}$ plus 0.35 $m^3 s^{-1}$ from the Arnera). This was rather a low value with respect to the mean (i.e., 2.30 $m^3 s^{-1}$ for pre-dam data; 2.19 $m^3 s^{-1}$ for complete data series). Specific flow discharge (Q_s) flowing into the reservoir averaged 11.2 and 5.8 $l s^{-1} km^{-2}$ for the $Muga_{up}$ and the Arnera respectively.

The $Muga_{up}$ and the Arnera display a clear Mediterranean flow regime, with flow peaks in spring and autumn and dry periods in summer and winter (Fig. 3). Maximum hourly Q occurred in March 2013 with 353 $m^3 s^{-1}$ at EA050 and 144 $m^3 s^{-1}$ at EA051, which resulted in ca. 500 $m^3 s^{-1}$ entering the reservoir. However, the sum of both discharges at daily scale resulted in a total Q of 201 $m^3 s^{-1}$ (i.e., 138.5 and 62.5 $m^3 s^{-1}$ for EA050 and EA051 respectively), which is associated with a recurrence interval of 60 years according to the pre-dam records. The Q_c (maximum annual mean daily flow) of pre-dam years averaged 56 $m^3 s^{-1}$, while for the three study years mean Q_c equalled 93 $m^3 s^{-1}$. During the pre-dam period Q_c was > 200 $m^3 s^{-1}$ only

345 once, indicating the exceptional nature of the 6 March 2013 flood. In fact, only 8 days from the
346 > 17,000 days of pre-dam data recorded Q higher than 100 m^3 s^{-1}. Likewise, a total of 46 days
347 had Q > 50 m^3 s^{-1}, also indicating the unusual occurrence of the 2014-2015 peaks. Daily Q
348 coefficient of variation ($CV_Q = Q_{SD}/Q_{mean}$) was > 500%, indicating the very high variability of Q
349 during the study period.

350 Flood events were flashy, and Q peaks were reached in a few hours. High flows occurred for <
351 5% of the time (Fig. 4). Floods occurred mainly during autumn and the late winter-early spring
352 period. Three events had remarkable peak flows and runoff volume entering the reservoir and
353 occurred in the first and third years of the study period (Table 3). The second year was the driest
354 but had a large number of small floods.

355 *4.1.2. Suspended sediment transport and load*

356 Suspended sediment transport at EA050 equalled 7834 t, with notable variability between years
357 (i.e., 5492, 424, and 1918 t for the three consecutive years respectively). The EA051 showed a
358 similar temporal distribution of suspended sediment loads, although lower; there, the total
359 suspended load that passed through EA051 in the study period was 2445 t (i.e., 1809, 210, and
360 426 t for the three consecutive years respectively).

361 The relationship between Q and *SSC* indicated that the *SSL* generally is hydraulically dependant
362 in the two rivers (Table 1). Some floods, however, displayed independent relations between Q
363 and *SSC*, in which the maximum Q did not match the maximum *SSC* (Tables 2 and 3). In fact,
364 maximum *SSC* at EA050 and EA051 were measured on 31 October 2012 and 21 October 2012
365 respectively during low magnitude floods (Table 3) and exceeded 0.8 g l^{-1} in both cases.
366 Because hydrological and sedimentary data for the months before these events were not
367 available, the observed values cannot be fully explained. However, the high availability of
368 sediments after the low-flow summer period and the flashiness of autumn storms could justify
369 those values. This lack of relation between Q and *SSC* translated to the general runoff-*SSL*
370 relation and reduced its linearity (especially in the case of EA050; Table 1).

371 *4.1.3. Bedload transport and load*

372 Bedload transport in the $Muga_{up}$ responded to flow hydraulics as it was assessed by formulae.
373 Hence, bedload transport occurred exclusively during floods, and the number of floods and its
374 magnitude determined the amount of material transported as bedload. The total bedload
375 calculated for the study period was 7981 t, and the variability between years was high (Table 4).
376 The 2013-2014 year (when no high floods occurred) showed negligible bedload transport (i.e.,
377 28.7 t), while the other two years had higher floods that also transported higher loads (i.e.,
378 between 3000 and 5000 t respectively; Table 4).

379 Although the discrepancy in bedload transport values predicted by the two formulae may seem
380 high, this difference can be considered small for gravel-bed rivers (e.g., Habersack and Laronne,
381 2002; Barry et al., 2008; López et al., 2014, 2015), especially for armoured river beds. The
382 highest rates estimated for EA050 correspond with peak *Q;* i.e., the highest rates were obtained
383 for the 6 March 2013 flood and equalled 14.1 and 17.3 kg s^{-1} m^{-1} for Recking (2010) and
384 Bathurst (2007) respectively. For the second largest flood, the maximum bedload transport rate
385 was 7.6 kg s^{-1} m^{-1} for Recking (2010) and 8.7 kg s^{-1} m^{-1} for Bathurst (2007). As previously
386 mentioned, Recking (2010) is a nonthreshold equation. In our study, the formula predicted low
387 rates of bedload transport when the amour layer was not yet broken (i.e., < 0.1 kg s^{-1} m^{-1}). These
388 low values likely correspond to the movement of fine sediments over the unbroken armour
389 layer, and can be considered marginal bedload. In fact, it represented < 1.5% of the predicted
390 total bedload transport. The Bathurst formula has been applied assuming that, if the armour is
391 not disturbed, bedload transport is zero. Worth to note that, in the 6 March 2013 flood,
392 maximum bedload rates for EA050 did exceed the maximum calibration and validation values
393 used to develop the applied formulae. This occurred for a total of 6 hours and under intense
394 flow conditions, a fact that may have overestimated bedload calculations. According to field
395 observations, and despite the armour layer, the nine floods that occurred during the study period
396 had sufficient competence to mobilise sediment particles or, at least, winnow the upper layer of
397 the bed. Mobility predicted by the equations coincides with field observations on tracers'

mobility, thus the breaking up of the armour layer. Although a clear threshold could not be established for particle entrainment, observations showed that 3 m^3 s^{-1} were sufficient to mobilise particles up to 36 mm. Scour chains indicated a notable dynamism of the active layer, reaching values > 25-30 cm for the largest floods. The thickness of the active layer seemed to be, *a priori*, related to the peak *Q*, but it is not possible to establish a pattern of erosion or aggradation. The GSD corroborate that sediments could be easily mobilised under relatively high floods and were smaller than the estimated thickness of the active layer.

The Arnera subbasin showed less variability between years, with bedload around 1500-1800 t a^{-1} (Table 4), transporting a total of 4815 t during the whole study period. Sands in the Arnera mobilised at lower *Q* than in the $Muga_{up}$ because of the high shear stress attained in the narrow study section, altogether favouring a more constant bedload transport. There, bedload was limited by the availability of sediments before the flood and by the presence of bedrock, with likely all sediments present in the bed mobilising during large floods.

4.1.4. Total sediment load

Tables 2 and 4 summarise the sediment transport in the two streams. The total sediment load (hereafter *TSL*) carried by the two streams for the whole study period amounted to 23,074 t, yielding an annual mean of 7691 t (i.e., 13,956, 2121, and 6997 t for the three consecutive years respectively). The total load represents a specific sediment yield of 63 t km^{-2} a^{-1} for the $Muga_{up}$ and 40 t km^{-2} a^{-1} for the Arnera. In the particular case of the Arnera, the lower sediment yield together with the observed breakpoint in the *Q*-*SSC* relation (Fig. 2) could indicate that it acted as a supply-limited system, with sediment exhaustion above ~10 m^3 s^{-1}. Overall, values in the upper Muga are within the range of those estimated in the Mediterranean basins of the Iberian Peninsula (e.g., Poesen and Hooke, 1997; Liquete et al., 2009; Buendia et al., 2016) and also similar to those estimated for Mediterranean basins in the south of France (Têt: 40 t km^{-2} a^{-1}, Serrat et al., 2001; and Agly: 130 t km^{-2} a^{-1}, Serrat, 2000). However, these values are lower than those obtained in other Mediterranean regions, as in the upper Celone River (250-384 t km^{-2} a^{-1},

De Girolamo et al., 2015) or the estimated values for the eastern and southern parts of the Mediterranean basin (i.e., 315 t km^{-2} a^{-1} for Greece and Turkey; 1400 t km^{-2} a^{-1} for Croatia and Albania; 325 t km^{-2} a^{-1} for North Africa; Poulos and Collins, 2002). Despite these regional values, other studies reported much lower values, e.g., Van Rompaey et al. (2005) for several small to medium-scale Italian basins.

Up to 55% of the *TSL* upstream from the reservoir (i.e., 12,796 t) was transported as bedload (*BL*), while the remaining 10,278 t were transported in suspension (suspended sediment load, *SSL*). The $Muga_{up}$ subbasin accounted for the 76% of the *SSL* and the 62% of the *BL* of the *TSL* (i.e., 7834 and 7981 t respectively), whereas the Arnera yielded the remaining amount (i.e., 2445 t as *SSL* and 4815 t as *BL*). The percentage of bedload transport in the $Muga_{up}$ subbasin (i.e., 50%) lies within the upper limit of other Mediterranean catchments (e.g., 8.3% for Nahal Estemoa and 68% for Nahal Yael, Powell et al., 1996). In the Arnera, bedload transport accounted for 66% of the *TSL* of the subbasin, a value similar to those found in other rivers flowing on sand beds (e.g., 67% in Arbúcies, Batalla and Sala, 1996; and 80% for the River Tordera, Rovira et al., 2005a and b). Both *SSL* and *BL* showed high interannual variability.

The $Muga_{up}$ is a clear example on how the proportion of *BL* and *SSL* responds to specific hydrological characteristics: the proportion of *SSL* and *BL* was similar for the first year, *BL* was considerably higher in the third year (when two large floods occurred), and *SSL* was predominant in the second year when only small low-competent events took place. In contrast, the Arnera showed similar loads in suspension and bedload for 2012-2013, while *BL* was considerably higher than *SSL* in the other two years. This may be related to the high mobility of the sandy sediments present in the bed. Batalla et al. (1995) found that bedload was double the suspended load in rivers dominated by sand fractions in the river bed, while Turowsky et al. (2010) observed that bedload in this type of river could attain up to 50% of the total load, much higher than that usually observed in gravel-bed rivers.

449 Runoff and sediment load frequency curves (Fig. 5) showed a similar behaviour between the
450 two basins. The steep slope of frequency curves is characteristic of Mediterranean rivers (e.g.,
451 Vericat and Batalla, 2010; Lobera et al., 2016) and indicate that most of the load occurs during
452 short periods of time (floods). At EA050, years 2012-2013 and 2014-2015 registered at least
453 one large flood (> 100 $m^3 s^{-1}$) that carried large volumes of water and sediments, while during
454 2013-2014 all floods were < 25 $m^3 s^{-1}$. Upstream from the dam (i.e., EA050 + EA051), the years
455 2012-2013 and 2014-2015 had 90% of the total runoff occurring in 50% of the year, whereas
456 90% of the *SSL* was transported by *Q* occurring < 1% of the time. In contrast, curves indicate a
457 slightly more constant sediment load during 2013-2014. Bedload curves could only be drawn
458 for the $Muga_{up}$. They indicated that the 90% of the bedload was transported in < 0.5% of the
459 time, indicating the higher dependency of *BL* on flood competence (i.e., energy expenditure in
460 the channel) in comparison to that needed to transport *SSL*. As a summary, *Q* equalled or
461 exceeded 3% of time and was responsible for ca. 50% of the runoff but for > 95% of the *SSL*
462 and > 99.5% of the *BL*. Frequency curves for EA050 indicate a difference between years; there,
463 50% of the runoff occurred ~ 15% of the time in the very dry year (i.e., 2013-2014), but only
464 5% of the time in the dry years. The 90% of runoff occurred in 55% and 75% of the time for dry
465 and very dry years respectively. In EA051 half of the runoff occurred < 20% of the time, while
466 90% occurred between 60 and 75% of the time, altogether indicating a relatively more regular
467 flow regime. The *SSL* curve showed that 50% of the load was transported in < 0.3% of the time,
468 whereas 90% occurred in < 3% of the time. A single flood can contribute with almost half of the
469 runoff of the whole year (Table 3) and a considerable part of the annual *SSL* (50-95%). The *BL*
470 duration could not be assessed by frequency curves, but it probably was more constantly
471 provided than in EA050 (i.e., sands need relatively low discharges to entrain). Overall, results in
472 the upper Muga are analogous to those obtained in the nearby River Têt (northern Pyrenees) or
473 the upper River Celone (central Italy), where a very high proportion of sediments were
474 transported during high flows or floods (Serrat et al., 2001; De Girolamo et al., 2015).

475 Summarizing, the high time-concentration of sediment transport events in a few hours/days
476 shown in frequency curves indicate that floods are determinant for sediment transport. Hence,
477 the number of floods is a key factor to explain the magnitude and duration of the sediment load.
478 Additionally, as suspended sediment and bedload transport are hydraulically dependent, the
479 magnitude of the floods is also a very important factor to explain the temporal distribution of
480 the sediment loads.

481 *4.2. Flow and sediment load downstream from the dam*

482 *4.2.1. Hydrology and runoff*

483 Downstream from the dam runoff was also below the long-term average: mean annual runoff
484 32.4 *vs.* 62.6 hm^3 post-dam data (i.e., 1970-2011) and 69.2 hm^3 complete data series (i.e., 1912-
485 2011). Mean Q at EA012 for the whole study period was 1.03 $m^3 s^{-1}$, considerably lower than
486 the long-term values (i.e., 1.98 $m^3 s^{-1}$ for post-dam data; 2.19 $m^3 s^{-1}$ for complete data series).
487 Mean Q was slightly lower than upstream and also displayed less temporal variability (i.e., as
488 indicated by the *SD* of the discharges; see Table 1). At the daily scale, the variability was lower
489 at EA012 (daily CV_Q = 108%) than upstream. Both metrics reflect the effect of regulation on the
490 river flow regime. Maximum hourly Q occurred in March 2013 with a flood peak of 41.3 $m^3 s^{-1}$,
491 while maximum daily Q equalled 12.3 $m^3 s^{-1}$, which corresponded to a recurrence interval of 1.4
492 years, according to post-dam data. The average of the post-dam Q_c data was 24.7 $m^3 s^{-1}$, while
493 for the three study years mean Q_c downstream from the dam equalled 5.5 $m^3 s^{-1}$. During post-
494 dam years, mean daily Q was > 50 $m^3 s^{-1}$ that occurred in 5 floods (13 days out of 13,819 of
495 available records), with Q > 10 $m^3 s^{-1}$ in 157 days. These results, together in the differences with
496 data upstream from the dam, point out the dryness downstream. Dams exert a role as controllers
497 of the hydrological regime even during large floods (i.e., reservoir management and dam
498 operation work together to route, reduce, or even *eliminate* flood peaks). Additionally, in
499 contrast to sections upstream, minimum flows did not occur in summer, when water releases

500 from the reservoir for agricultural and tourism uses occurs, but in winter in a sort of inversion of
501 the hydrological regime (Piqué et al., 2016).

502 Flow duration curves (Fig. 4) reflect the regulation effect of reservoirs and water withdrawals
503 (Magilligan and Nislow, 2005). Duration of high flows in the Muga below the dam were
504 reduced whereas low flows were increased, resulting in a more constant flow regime than
505 upstream. Breakpoints between 0.5 and 1 $m^3 s^{-1}$ in the duration curves (Fig. 4) corresponded to
506 sudden changes in flow for irrigation releases from the dam. Median Q was lower downstream
507 from the dam, although the difference with upstream was small. The Q_{P95} and Q_{P99} showed the
508 lower magnitude and frequency of floods in relation to the same upstream flow percentiles. Not
509 all floods occurring upstream from the reservoir occurred at EA012, and only three flood
510 episodes reached higher Q than those released during summer months. The larger floods
511 coincided with upstream episodes capable of filling up the reservoir (i.e., to 95%), and probably
512 respond to operative water releases. This caused the reduction of flood lamination capacity of
513 the reservoir just before the irrigation season. Compared to upstream, the magnitude and
514 duration of these floods was reduced at EA012 and had different hydrograph shapes (Fig. 3).

515 *4.2.2. Suspended sediment transport and load*

516 The total suspended sediment load at EA012 for the whole study period was 800 t, a value that
517 represents an annual mean of 267 t (i.e., 390, 171, and 239 t for the three consecutive years,
518 respectively).

519 The *SSC* at EA012 was not Q dependent, with higher values of *SSC* not corresponding to higher
520 flows (Fig. 2). Sediment in suspension was only carried during floods, while high discharges
521 (i.e., > 3 $m^3 s^{-1}$) were usually clear and with low *SSC* (< 10 mg l^{-1}). Maximum instantaneous *SSC*
522 was 0.6 g l^{-1}, during the 29 September 2014 flood and did not coincide with the maximum Q
523 (Table 2). Maximum *SSC* values were lower than those measured upstream.

524

525 *4.2.3. Bedload transport and load*

526 Bedload transport was predicted only for the higher *Q* of the 6 March 2013 flood and lasted for
527 16 hours. The maximum rates predicted for the period of armour breakup were estimated at 1.6
528 and 0.26 kg s^{-1} m^{-1}, using Recking (2010) and Bathurst (2007) respectively. These rates are 8 to
529 66 times lower than those estimated for $Muga_{up}$ using the same formulae, and indicate that
530 although the armour downstream of the dam probably broke during the 6 March 2013 flood, the
531 magnitude and duration of the bedload transport were very low downstream. According to the
532 predictions of the mentioned formulae, the armour layer remained stable the rest of the time and
533 no particle movement was observed. The high degree of armouring, together with the particle
534 size of the surface layer, ensured bed stability.

535 In general, predictions of bedload equations were consistent with the observations from tracers,
536 and no mobility was observed while they were installed. Notably, however, particle movement
537 during the largest flood (i.e., 6 March 2013) could not be verified as tracers were not already
538 installed. Despite this, and because of the short duration of the episode and the low predicted
539 bedload rates, bedload can be considered negligible for the purpose of this work.

540 *4.2.4. Total sediment load*

541 As stated, *SSL* constituted the total load passing through the EA012 monitoring station (Fig. 6),
542 so ca. 800 t were transported downstream from the dam.

543 The *SSL* curve is less steep than upstream, indicating that suspended sediment passing through
544 the EA012 was transported more constantly (Fig. 5). The 50% of the *SSL* was transported
545 between 13 and 15% of the time (depending on the year), while 90% of the sediment was
546 transported between 43 and 48% of the time. Similar suspended sediment frequency curves
547 were observed below dams at the lower Ebro (Tena et al., 2012).

548 Results indicate that the factors controlling the sediment transport downstream from dams are
549 substantially different from those observed upstream; 'high flows' are not directly responsible

550 for sediment transport at EA012 because of the existence of an armoured river bed and owing to
551 the operational needs of the dam.

552 *4.3. The role of the dam in the Upper Muga sediment budget*

553 Figure 6 shows the seasonal and the annual water and sediment budgets for the upper River
554 Muga. Overall, the year 2012-2013 contributed the most, in terms of water and sediment load.
555 For the complete study period, most of the total load upstream from the dam was supplied by
556 the $Muga_{up}$ subbasin, yielding 69% of *TSL* to the reservoir (i.e., 15,815 out of 23,074 t). At the
557 annual scale, the contribution of each subbasin varied considerably. The $Muga_{up}$ yielded > 70%
558 of the *TSL* to the reservoir for the years 2012-2013 and 2014-2015, but the Arnera transported
559 more sediment in 2013-2014 (i.e., 79% of the *TSL*). This is probably related to the sediments
560 transported as bedload under low flows during that very dry year. Sands from the Arnera needed
561 less competence to mobilise, so small floods during 2013-14 were likely capable of mobilising
562 the sandy bed material of the Arnera but not the gravels in the $Muga_{up}$. However, in the 2012-
563 2013 and 2014-2015 large floods broke the armour layer and mobilised sediments in the $Muga_{up}$
564 subbasin, so the contribution of that river as bedload was substantially higher. Seasonal
565 hydrological or sedimentary patterns were not apparent, showing that individual floods control
566 mass production in the catchments regardless of the season in which they occur.

567 The *TSL* was reduced considerably below the dam, a fact that reflects the role of the reservoir in
568 trapping sediments. The reduction of sediment transport downstream is > 95%. This value is
569 much higher than the mean reduction estimated for the northwestern Mediterranean region (i.e.,
570 56%; Poulos and Collins, 2002) and for southwestern Europe (e.g., > 50%; Vörösmarty et al.,
571 2003). The retention capacity of reservoirs estimated in the Muga by means of the Heinemann
572 method (observed/predicted sediment loads upstream and downstream from the dam;
573 Heinemann, 1981) was 86% for fine sediments (94.7%, 73.0%, and 89.8% for consecutive
574 years), while, as acknowledged, bedload retention was total. This implied the retention of a total
575 of 9478 t of suspended sediment, in addition to the 12,796 t carried as bedload (Table 5) for the

576 complete 2012-2015 study period. The suspended sediment trapping efficiency of the Darnius-
577 Boadella Reservoir fits in the mid-upper range of the values found in the literature. Our data are
578 higher than those of the Lacang River Dam, China (Fu and He, 2007; with 60% trapping) and
579 similar to those from several dams in Sebou and Moulouya Rivers, Morocco, and in Smoky Hill
580 and Big Blue Rivers, USA (Snoussi et al., 2001; Juracek, 2011; with trapping efficiencies >
581 90%).

582 The sediment transported downstream from the dam could come from reservoir releases as well
583 as from the drainage area between the dam and the EA012 monitoring station. The mean
584 sedimentation rate obtained using the two available bathymetries from the Catalan Water
585 Agency for the reservoir performs higher than our estimations (i.e., 70,000 t a^{-1}). The reason for
586 this difference may be the dry character of the study years, a fact that likely underestimated the
587 mean total load usually transported by the two upstream rivers. Errors arising from calculation
588 of river total sediment load and extrapolations typically associated with bathymetric surveys
589 may have enhanced this discrepancy.

590 *4.4. Downstream Implications of the Darnius-Boadella Reservoir*

591 Although sedimentation does not seem to threaten the lifetime of the Darnius-Boadella
592 Reservoir, it does have consequences in the downstream river reaches as a result of the acute
593 sediment deficit. River sediments constitute the habitat of benthic biota and are the refuge for
594 invertebrates and fish, so the lack of river bed mobility and the lack of sediment coming from
595 upstream alter the sedimentary and ecological equilibrium of the fluvial system. The physical
596 effects of the reduction in sediment transport downstream from dams was already described by
597 Williams and Wolman (1984), and effects on invertebrate diversity and density were also
598 established (Petts et al., 1993). Other early studies (e.g., Kellerhals and Gill, 1973; Kondolf and
599 Matthews, 1993) described and compiled (respectively) the morphological changes that occur
600 downstream from dams caused by sediment deficit: i.e., bed material coarsening, river bed
601 incision, or changes in channel geometry. Our study shows that the River Muga downstream

602 from the Darnius-Boadella Dam is highly armoured, probably as a consequence of the reported
603 sediment deficit but also because of the existence of sufficient competent floods to mobilise
604 material downstream (Schmidt and Wilcock, 2008). Hence, although floods are not highly
605 recurrent in the Muga downstream from the dam as a result of the high control of flow
606 discharges, when they occur they did contribute to the coarsening of the river bed and the
607 formation of an armour layer.

608 The inherent capacity of a river to recover from dam effects depends mainly on the downstream
609 distance and the number and capacity of tributaries it receives; without these influents, river
610 degradation may remain for a long distance (e.g., Chien, 1985). Although we only considered
611 the upper part of the catchment, Piqué et al. (2016) observed that the Muga only recovers a
612 certain degree of hydrological dynamism in the lowermost reach, where the river is close to the
613 sea. Examples such as the River Muga, where dam effects are observed farther downstream,
614 revealing the need that practices to reduce sediment deficit so as to rehabilitate sedimentary
615 fluvial dynamics downstream from large dams should be considered in reservoir managing
616 operations, and periodically implemented (e.g., Owens et al., 2005). These operations should be
617 based on accurate sediment budgets and load estimations. In Mediterranean regions the need for
618 long-term water storage to reduce inherent hydroclimatic variability complicates the
619 implementation of feasible alternatives for sound sediment management to mitigate the lack of
620 sediments downstream from dams, such as sediment bypassing, sediment pass-through, and off-
621 channel reservoir storage, among others (e.g., Kondolf et al., 2014). However, other practices
622 can still be used in the downstream channel, such as regular reservoir dredging, feeding
623 sediment injection, and gravel augmentation actions. Despite the difficulties to overcome the
624 sediment deficit caused by dams, management actions may ameliorate it and add dynamism to
625 the river. As an example, flushing flows are controlled flow releases and have been used
626 worldwide as a restoration practice to maintain or improve water quality and river ecosystem
627 functioning (e.g., Canada, BC Hydro, 1996; USA, Kondolf, 1998; Sri Lanka, Acreman, 2000;
628 China, Yellow River Conservancy Commission, 2004). These also have been implemented in

629 Mediterranean rivers with the purpose of reactivating the river bed and controling macrophyte
630 growth (Batalla and Vericat, 2009). This type of rehabilitation action also could be implemented
631 in the River Muga. As flushing flows would not entirely solve sediment deficit downstream
632 from the dam, other (costly) actions such as gravel augmentation would be implemented. Prior
633 to these, specific ecological targets should be defined to attain a comprehensive river
634 management plan.

635 **5. Conclusions**

636 The sediment budget of the upper River Muga is a result of the natural high spatial and temporal
637 variability of sediment transport in rivers of the Mediterranean region as well as of the local
638 effect of the dam. This 3-year budget has identified clear differences between sediment transport
639 modes (suspended and bedload), between river sections, and between years owing to different
640 hydrology and, most remarkably, to the characteristics of river bed material. In particular:

641 • Almost 23,000 t of sediments were transported to the Darnius-Boadella Reservoir during the
642 2012-2015 hydrological years: 55% as bedload and the rest in suspension. The $Muga_{up}$
643 subbasin contributed with two-thirds of the load, owing to its larger contribution area, runoff
644 volumes and magnitude of flood peaks.
645 • The sediment load of the upper River Muga depends mainly on large floods, as indicated by
646 the steepness of the load duration curves, while low flows do not contribute to sediment
647 transport. Small and medium events had very little effect in the gravel-bed River Muga but
648 can carry high sediment loads in the sand river Arnera. However, the high inter- and intra-
649 annual temporal variability made it difficult to predict their precise role on the long-term
650 sediment load of the river.
651 • Almost all the suspended sediment load was trapped by the Darnius-Boadella Dam, and this
652 caused an acute sediment deficit downstream. Although the reservoir trapping efficiency is
653 very high, sediment yield calculations together with long-term data from bathymetries
654 showed that the storage capacity of the reservoir has not been dramatically reduced since

655 dam construction. This can be attributed to the extraordinary large reservoir volume in
656 comparison to the annual runoff of the catchment and the moderate load supply from these
657 two headwater forested catchments. The mean annual reduction of reservoir capacity during
658 the study period has been estimated at 0.01%, well below regional values.

659 This study illustrates the alteration of sediment transport derived from dam construction in a
660 mesoscale Mediterranean river. The River Muga is an example of a dammed river subjected to
661 marked Mediterranean climate, with high intra- and interannual hydroclimatic variability. The
662 Muga can be considered representative of the mid-latitude mesoscale coastal Mediterranean
663 catchments in terms of annual precipitation, temperature, runoff, and percentage of irrigated
664 area (PERSEUS-UNEP/MAP Report, 2015). Hence, despite the inherent high variability, this is
665 a good example illustrating the current hydrosedimentary situation of many Mediterranean
666 rivers. The extrapolation of the information obtained from this work, together with other studies
667 related to the reduction of sediment delivered to the oceans (e.g., Milliman, 2001), is evidence
668 of the need of management actions to improve the functioning of fluvial ecosystems, despite
669 other actions specifically designed according to their biophysical characteristics and water uses.

670 **Acknowledgements**

671 This research was developed in the frame of the project 'SCARCE Consolider Ingenio 2010
672 CSD2009-00065(2009-2014)' funded by the Spanish Ministry of Economy and
673 Competitiveness. Authors acknowledge the support from the Economy and Knowledge
674 Department of the Catalan Government through the Consolidated Research Groups: Fluvial
675 Dynamics Research Group (2014 SGR 645) and the Catalan Institute for Water Research (2014
676 SGR 291). The authors would like to thank the Catalan Water Agency for allowing the
677 installation of measuring equipment in the Muga gauging stations and for providing
678 hydrological data, as well as the Meteorological Service of Catalonia and two private owners for
679 supplying precipitation data. Part of the water stage and turbidity probes was funded jointly by
680 the European Regional Development Fund and the Spanish Ministry of Science and Innovation.

681 The authors are especially indebted to Carmen Gutiérrez and Alvaro Tena for their assistance
682 during fieldwork. We thank Mark Smith for the English revision of the manuscript. Reviews by
683 the editor and anonymous reviewers greatly improved the final version of the manuscript.

684 **REFERENCES**

685 Acreman, M. 2000. Managed Flood Releases from Reservoirs: Issues and Guidance. World
686 Commission of Dams Thematic Review: II-1. Centre for Ecology and Hydrology, Wallingford,
687 UK, 88 pp.

688 Barry, J.J., Buffington, J.M., Goodwin, P.G., King, J.G., Emmett, W.W., 2008. Performance of
689 bed-load transport equations relative to geomorphic significance: predicting effective discharge
690 and its transport rate. Journal of Hydraulic Engineering 134(5), 601-615. doi:
691 10.1061/(ASCE)0733-9429(2008)134:5(601)

692 Batalla, R.J., 1997. Evaluating bed-material transport equations using field measurements in a
693 sandy gravel-bed stream, Arbúcies River, NE Spain. Earth Surface Processes and Landforms
694 22, 121-130. doi: 10.1002/(SICI)1096-9837(199702)22:2<121::AID-ESP671>3.0.CO;2-7

695 Batalla, R.J., Sala, M., 1996. Impact of land-use practices on the sediment yield of a partially
696 disturbed Mediterranean catchment. Zeitschrift fur Geomorphologie Supplementband 107, 79-
697 93.

698 Batalla, R.J., Vericat, D., 2009. Hydrological and sediment transport dynamics of flushing
699 flows: implications for management in large Mediterranean rivers. River Research and
700 Applications 25, 297-314. doi: 10.1002/rra.1160

701 Batalla, R.J., Vericat, D., 2013. River's Architecture Supporting Life. In: Elosegui, A., Sabater,
702 S. (Eds.), River Conservation: Challenges and Opportunities. Fundación BBVA, Madrid, Spain,
703 pp. 61-75.

704 Batalla, R.J., Sala, M., Werritty, A., 1995. Sediment budget focused on solid material transport
705 in a subhumid Mediterranean drainage basin. Zeitschrift für Geomorphologie 39(2), 249-264.
706 doi: 0372-8854/94/0249

707 Batalla, R.J., Gomez, C.M., Kondolf, G.M., 2004. Reservoir-induced hydrological changes in
708 the Ebro River basin, NE Spain. Journal of Hydrology 290, 117-136. doi:
709 10.1016/j.jhydrol.2003.12.002

710 Bathurst, J.C., 2007. Effect of Coarse Surface Layer on Bed-Load Transport. Journal of
711 Hydraulic Engineering 133, 1192-1205. doi: 10.1061/(ASCE)0733-9429(2007)133:11(1192)

712 BC Hydro, 1996. The Alouette Stakesholder Committee Process, Analysis and
713 Recommendations, 54 pp.

714 Beaumont, P., 1978. Man's impact on river systems: a world-wide view. Area 10, 38-41.

715 Billi, P., 2011. Flash flood sediment transport in a steep sand-bed ephemeral stream.
716 International Journal of Sediment Research 26(2), 193-209. doi: 10.1016/S1001-
717 6279(11)60086-3

718 Brown, C.B., 1950. Sediment transportation. In: Rouse, H. (Ed.), Engineering Hydraulics.
719 Wiley, New York, pp. 769-857.

720 Buendia, C., Gibbins, C.N., Vericat, D., Batalla, R.J., 2014. Effects of flow and fine sediment
721 dynamics on the turnover of stream invertebrate assemblages. Ecohydrology 7(4), 1105-1123.
722 doi: 10.1002/eco.1443

723 Buendia, C., Herrero, A., Sabater, S., Batalla, R.J., 2016. An appraisal of the sediment yield in
724 western Mediterranean river basins. Science of the Total Environment 572, 538-553. doi:
725 10.1016/j.scitotenv.2016.08.065

726 Chien, N., 1985. Changes in river regime after the construction of upstream reservoirs. Earth
727 Surface Processes and Landforms 10, 143-159. doi: 10.1002/esp.3290100207

728 Church, M., McLean, D.G., Wolcott, J.F., 1987. River bed gravels: sampling and analysis. In:
729 Thorne, C.R., Bathurst, J.C., Hey, R.D. (Eds.), Sediment Transport in Gravel-bed Rivers. John
730 Wiley and Sons, Chichester, UK, pp. 43-88.

731 Church, M., Biron, M., Roy, A., 2012. Gravel-bed Rivers: Processes, Tools, Environments.
732 Wiley-Blackwell, 580 pp.

733 De Girolamo, A.M., Pappagallo, G., Lo Porto, A., 2015. Temporal variability of suspended
734 sediment transport and rating curves in a Mediterranean river basin: The Celone (SE Italy).
735 Catena 128, 135-143. doi: 10.1016/j.catena.2014.09.020

736 Dietrich, W., Dunne, T., 1978. Sediment budget for a small catchment in mountainous terrain.
737 Zeitschrift für Geomorphologie N.F. Supplement Band 29, 191-206.

738 Dietrich, W. E., Dunne, T., Humphrey, N.F., Reid, L.M., 1982. Construction of sediment
739 budgets for drainage basins. In: Sediment Budgets and Routing in Forested Drainage Basins.
740 General Technical Report PNW-141. U.S.D.A. Forest Service, Portland, pp. 5-23.

741 Downing, J., 2006. Twenty-five years with OBS sensors: The good, the bad, and the ugly.
742 Continental Shelf Research 26(17-18), 2299-2318.

743 Draut, A., Logan, J.B., Mastin, M.C., 2011. Channel evolution on the dammed Elwha River,
744 Washington, USA. Geomorphology 127, 71-87. doi: 10.1016/j.geomorph.2010.12.008

745 Drever, J.I., 1982. The geochemistry of natural waters. Prentice Hall, Englewood Cliffs, 388 pp.

746 Farley, D.A., Werritty, A., 1989. Hydrochemical budgets for the Loch Dee Experimental
747 Catchments, Southwest Scotland (1981-1985). Journal of Hydrology 109(3-4), 351-368. doi:
748 10.1016/0022-1694(89)90024-3

749 Fu, K., He, D., 2007. Analysis and prediction of sediment trapping efficiencies of the reservoirs
750 in the mainstream of the Lancang River. Chinese Science Bulletin 52(Suppl 2), 134-140. doi:
751 10.1007/s11434-007-7026-0

752 Gallart, F., Balasch, J. C, Regüés, D., Soler, M., Castelltort, X., 2005. Catchment Dynamics in a
753 Mediterranean Mountain Environment. The Vallcebre Research Basins (Southeastern Pyrenees).
754 In: Garcia, C., Batalla, R.J. (Eds.), Catchment Dynamics and River Processes: Mediterranean
755 and Other Climate Regions. Elsevier, Amsterdam, pp. 17-29. doi:10.1016/S0928-
756 2025(05)80008-2.

757 García-Ruiz, J.M., Arnáez, J., Beguería, S., Seeger, M., Martí-Bono, C., Regüés, D., Lana-
758 Renault, N., White, S., 2005. Runoff generation in an intensively disturbed, abandoned
759 farmland catchment, Central Spanish Pyrenees. Catena 59, 79-92. doi:
760 10.1016/j.catena.2004.05.006

761 García-Ruiz, J.M., Nadal-Romero, E., Lana-Renault, N., Beguería, S., 2013. Erosion in
762 Mediterranean landscapes: Changes and future challenges. Geomorphology 198, 20-36. doi:
763 10.1016/j.geomorph.2013.05.023

764 Gomez, B., Church, M., 1989. An assessment of bedload sediment transport formulae for gravel
765 bed rivers. Water Resources Research 25(6), 1161-1186. doi: 10.1029/WR025i006p01161

766 González-Hidalgo, J.C., Peña-Monné, J.L., de Luis, M., 2007. A review of daily soil erosion in
767 Western Mediterranean areas. Catena 71, 193-199. doi: 10.1016/j.catena.2007.03.005

768 Gonzalez-Hidalgo, J.C., Batalla, R.J., Cerda, A., 2013. Catchment size and contribution of the
769 largest daily events to suspended sediment load on the continental scale. Catena 102, 40-45. doi:
770 10.1016/j.catena.2010.10.011

771 Goodwin, P., Jorde, K., Meier, C., Parra, O., 2006. Minimizing environmental impacts of
772 hydropower development: transferring lessons from past projects to a proposed strategy for
773 Chile. Journal of Hydroinformatics 8(4), 253-270. doi: 10.2166/hydro.2006.005
774

775 Graf, W.L., 2006. Downstream hydrologic and geomorphic effects of large dams on American
776 rivers. Geomorphology 79, 336-360. doi: 10.1016/j.geomorph.2006.06.022

Habersack, H., Laronne, J.B., 2002. Evaluation and improvement of bed load discharge formulas based on Helley–Smith sampling in an Alpine gravel bed river. Journal of Hydraulic Engineering 128(5), 484-499. doi: 10.1061/(ASCE)0733-9429(2002)128:5(484)

Hamamori, A., 1962. A Theoretical Investigation on the Fluctuations of Bedload Transport. Delft Hydraulics Laboratory Report, R4. Delft, the Netherlands, 21 pp.

Harrelson, C.C., Rawlins, C.L., Potyondy, J.P., 1994. Stream Channel Reference Sites: an illustrated guide to field technique. General Technical Report RM-245, Department of Agriculture, Forest Service, Rocky Mountain Forest and Range Experiment Station. Fort Collins, CO, US, 61 pp.

Hassan, M. A., 1990. Scour, fill, and burial depth of coarse material in gravel bed streams. Earth Surface Processes and Landforms 15, 341-356. doi: 10.1002/esp.3290150405

Heinemann, H.G., 1981. A new sediment trap efficiency curve for small reservoirs. Water Resources Bulletin 17(5), 825-830. doi: 10.1111/j.1752-1688.1981.tb01304.x

Hubbell, D.W., 1987. Bedload sampling and analysis. In: Thorne, C. R., Bathurst, J. C., Hey, R. D. (Eds.), Sediment Transport in Gravel-bed Rivers, John Wiley & Sons, Chichester, UK, pp. 89-120.

Inbar, M., 1992. Rates of Fluvial Erosion in Basins with a Mediterranean Type Climate. Catena 19(3-4), 393-409. doi: 10.1016/0341-8162(92)90011-Y

Juracek, K.E., 2011. Suspended-sediment loads, reservoir sediment trap efficiency, and upstream and downstream channel stability for Kanopolis and Tuttle Creek Lakes, Kansas, 2008-10: U.S. Geological Survey Scientific Investigations Report 2011-5187, 35 pp.

799 Kellerhals, R., Gill, D., 1973. Observed and potential downstream effects of large storage
800 projects in Northern Canada. In: International Commission on Large Dams, Eleventh Congress,
801 Proceedings Vol 1, pp. 731-754.

802 Kesel, R.H., Yodis, E.G., Mc Craw, D.J., 1992. An approximation of the sediment budget of the
803 lower Mississippi River prior to major human modification. Earth Surface Processes and
804 Landforms 17, 711-722. doi: 10.1002/esp.3290170707

805 Kondolf, G.M., 1997. Hungry Water: Effects of Dams and Gravel Mining on River Channels.
806 Environmental Management 21(4), 533-551. doi: 10.1007/s002679900048

807 Kondolf, G.M., 1998. Lessons learned from river restoration projects in California. Aquatic
808 Conservation: Marine and Freshwater Ecosystems 8, 39-52. doi: 10.1002/(SICI)1099-
809 0755(199801/02)8:1<39::AID-AQC250>3.0.CO;2-9

810 Kondolf, G.M., Batalla, R.J., 2005. Hydrological Effects of Dams and Water Diversions on
811 Rivers of Mediterranean-Climate Regions: Examples from California. In: Garcia, C., Batalla,
812 R.J. (Eds.), Catchment Dynamics and River Processes. Mediterranean and Other Climate
813 Regions. Amsterdam, Elsevier, pp. 197-212. doi: 10.1016/S0928-2025(05)80017-3

814 Kondolf, G.M., Matthews, W.V.G., 1993. Management of Coarse Sediment in Regulated Rivers
815 of California. University of California, Water Resources Center, Davis, CA, USA, 128 pp.

816 Kondolf, G.M., Gao, Y., Annandale, G.W., Morris, G.L., Jiang, E., Zhang, J., Yongtao, C.,
817 Carling, P., Fu, K., Guo, Q., Hotchkiss, R., Peteuil, C., Sumi, T., Wang, H., Wang, Z., Wei, Z.,
818 Wu, B., Wu, C., Yang, C.T., 2014. Sustainable sediment management in reservoirs and
819 regulated rivers: Experiences from five continents. Earth's Future 2, 256-280.
820 doi:10.1002/2013EF000184

821 Leopold, L.B., Skibitzke, H.E., 1967. Observationson unmeasured rivers. Geografiska Annaler
822 49(2-4), 247-255.

823 Liquete, C., Canals, M., Ludwig, W., Arnau, P., 2009. Sediment discharge of the rivers of
824 Catalonia, NE Spain, and the influence of human impacts. Journal of Hydrology 366, 76-88.
825 doi: 10.1016/j.jhydrol.2008.12.013

826 Lobera, G., Batalla, R.J., Vericat, D., López-Tarazón, J.A., Tena A., 2016. Sediment transport
827 in two Mediterranean regulated rivers. Science of the Total Environment 540, 101-113. doi:
828 10.1016/j.scitotenv.2015.08.018

829 López, R., Barragán, J., Colomer, M.A., 2007. Flow resistance equations without explicit
830 estimation of the resistance coefficient for coarse-grained rivers. Journal of Hydrology 338,
831 113-121. doi:10.1016/j.jhydrol.2007.02.027

832 López, R., Vericat, D., Batalla, R.J., 2014. Evaluation of bed load transport formulae in a large
833 regulated gravel bed river. Journal of Hydrology 510, 164-181. doi:
834 10.1016/j.jhydrol.2013.12.014

835 López, R., Vericat, D., Batalla, R. J., 2015. Assessment of bed load transport formula for an
836 armoured gravel-bed river. Water Technology and Sciences 6(2), 5-20.

837 Lopez Saez, J., Corona, C., Stoffel, M., Rovéra, G., Astrade, L., Berger, F., 2011. Mapping of
838 erosion rates in marly badlands based on a coupling of anatomical changes in exposed roots
839 with slope maps derived from LiDAR data. Earth Surface Processes and Landforms 36(9),
840 1162-1171. doi: 10.1002/esp.2141

841 López-Tarazón, J.A., Batalla, R.J., Vericat, D., Francke, T., 2011. The sediment budget of a
842 highly dynamic mesoscale catchment: The River Isábena. Geomorphology 138(1), 15-28. doi:
843 10.1016/j.geomorph.2011.08.020

844 Loughran, R.J., Campbell, B.L., Shelly, D.J., Elliot, G.L., 1992. Developing a sediment budget
845 for a small drainage basin in Australia. Hydrological Processes 6, 145-158. doi:
846 10.1002/hyp.3360060203

847 Lucía, A., Recking, A., Martín-Duque, J.F., Storz-Peretz, Y., Laronne, J.B., 2013. Continuous
848 monitoring of bedload discharge in a small, steep sandy channel. Journal of Hydrology 497, 37-
849 50. doi: 10.1016/j.jhydrol.2013.05.034

850 Magilligan, F.J., Nislow, K.H., 2005. Changes in hydrologic regime by dams. Geomorphology
851 71, 61-78. doi: 10.1016/j.geomorph.2004.08.017

852 Merten, G.H., Capel, P.D., Minella, J.P.G., 2013. Effects of suspended sediment concentration
853 and grain size on three optical turbidity sensors. Journal of Soils and Sediments 14(7), 1235-
854 1241. doi: 10.1007/s11368-013-0813-0

855 Merz, J.E., Pasternack, G.B., Wheaton, J.M., 2006. Sediment budget for salmonid spawning
856 habitat rehabilitation in a regulated river. Geomorphology 76, 207-228. doi:
857 0.1016/j.geomorph.2005.11.004

858 Meybeck, M., 1983. Atmospheric inputs and river transport of dissolved substances.
859 Proceedings of the Hamburg Symposium. IAHS Publications 141, 173-192.

860 Milliman, J.D., 2001. Delivery and fate of fluvial water and sediment to the sea: a marine
861 geologist's view of European rivers. Scientia Marina 65(Suppl. 2), 121-132. doi:
862 10.3989/scimar.2001.65s2121

863 Minella, J.P.G., Merten, G.H., Reichert, J.M., Clarke, R.T., 2008. Estimating suspended
864 sediment concentrations and the calibration problem. Hydrological Processes 22(12), 1819-
865 1830. doi: 10.1002/hyp.6763

866 Nadal-Romero, E., González-Hidalgo, J.C., Cortesi, N., Desir, G., Gómez, J.A., Lasanta, T.,
867 Lucía, A., Marín, C., Martínez-Murillo, J.F., Pacheco, E., Rodríguez-Blanco, M.L., Romero
868 Díaz, A., Ruiz-Sinoga, J.D., Taguas, E.V., Taboada-Castro, M.T., Úbeda, X., Zabaleta, A.,
869 2015. Relationship of runoff, erosion and sediment yield to weather types in the Iberian
870 Peninsula. Geomorphology 228, 372-381. doi: 10.1016/j.geomorph.2014.09.011

871 Nawa, R. K., Frissell, C.A., 1993. Measuring Scour and Fill of Gravel Streambeds with Scour
872 Chains and Sliding-Bead Monitors. North American Journal of Fisheries Management 13, 634-
873 639. doi: 10.1577/1548-8675(1993)013<0634:MSAFOG>2.3.CO;2

874 Owens, P.N., Batalla, R.J., Collins, A.J., Gomez, B., Hicks, D.M., Horowitz, A.J., Kondolf,
875 G.M., Marden, M., Page, M.J., Peacock, D.H., Petticrew, E.L., Salomons, W., Trustrum, N.A.,
876 2005. Fine-grained sediment in river systems: environmental significance and management
877 issues. River Research and Applications 21, 693-717. doi: 10.1002/rra.878

878 PERSEUS-UNEP MAP Report, 2015. Atlas of Riverine Inputs to the Mediterranean Sea. 32 pp.

879 Petts, G., Armitage, P., Castella, E., 1993. Physical habitat changes and macroinvertebrate
880 response to river regulation: the River Rede, UK. Regulated Rivers: Research and Managament
881 8(1-2), 167-178. doi: 10.1002/rrr.3450080119

882 Piqué, G., Batalla, R.J., Sabater, S., 2016. Hydrological characterization of dammed rivers in
883 the NW Mediterranean region. Hydrological Processes 30, 1691-1707. doi: 10.1002/hyp.10728

884 Poesen, J.W.A., Hooke, J.M., 1997. Erosion, flooding and channel management in
885 Mediterranean environments of southern Europe. Progress in Physical Geography 21, 157-199.
886 doi: 10.1177/030913339702100201

887 Poulos, S.E., Collins, M.B., 2002. Fluviatile sediment fluxes to the Mediterranean Sea: a
888 quantitative approach and the influence of dams. In: Jones, S.J., Frostick, L.E. (Eds.), Sediment
889 Flux to Basins: Causes, Controls and Consequences. Geological Society, London, Special
890 Publications 191, 227-245.

891 Powell, D.M., Reid, I., Laronne, J.B., Frostick, L., 1996. Bed load as a component of sediment
892 yield from a semiarid watershed of the northern Negev. IAHS Publications 236, 389-397.

893 Powell, D.M., Brazier, R., Nichols, M., Wainwright, J., Parsons, A., 2003. Stream-bed Scour
894 and Fill in Low-order Ephemeral Stream Channels. Water Resources Research 41(5), 180-184.
895 doi: 10.1029/2004WR003662

896 Recking, A., 2010. A comparison between flume and field bed load transport data and
897 consequences for surface-based load transport prediction. Water Resources Research 46(3),
898 W03518. doi: 10.1029/2009WR008007

899 Recking, A., 2013. Simple Method for Calculating Reach-Averaged Bed-Load Transport.
900 Journal of Hydraulic Engineering 139, 70-75. doi: 10.1061/(ASCE)HY.1943-7900.0000653

901 Regüés, D., Nadal-Romero, E., 2013. Uncertainty in the evaluation of sediment yield from
902 badland areas: Suspended sediment transport estimated in the Araguás catchment (central
903 Spanish Pyrenees). Catena 106, 93-100. doi: 10.1016/j.catena.2012.05.006

904 Richards, K., 1982. Rivers: Form and Process in Alluvial Channels. Methuen, USA, 358 pp.

905 Rovira, A., Batalla, R.J., Sala, M., 2005a. Response of a river sediment budget after historical
906 gravel mining (the lower Tordera, NE Spain). River Research and Applications 21(7), 829-847.
907 doi: 10.1002/rra.885

908 Rovira, A., Batalla, R.J., Sala, M., 2005b. Fluvial sediment budget of a Mediterranean river: the
909 lower Tordera (Catalan Coastal Ranges, NE Spain). Catena 60, 19-42. doi:
910 10.1016/j.catena.2004.11.001

911 Sala, M. and Wheeler, D., 1988. Variación espacial de la carga de sedimentos en la cuenca del
912 río Tordera en condiciones de estiaje. Acta Geológica Hispánica 23(3), 209-216.

913 Schmidt, J. C., Wilcock, P.R., 2008. Metrics for assessing the downstream effects of dams,
914 Water Resources Research 44, W04404. doi:10.1029/2006WR005092.

915 Serrat, P., 2000. Genèse et dynamique d'un système fluvial méditerranéen: le bassin de l'Agly
916 (France). Ph. D. Dissertation, Université de Perpignan.

917 Serrat, P., Ludwig, W., Navarro, B., Blazi, J.L., 2001. Variabilité spatio-temporelle des flux de
918 matières en suspensión d'un fleuve côtier méditerranéen: la Têt (France). Earth and Planetary
919 Sciences 333, 389-397. doi: 10.1016/S1251-8050(01)01652-4

920 Shaw, E.M., 1983. Hydrology in Practice. Van Nostrand Reinhold, London, 539 pp.

921 Slaymaker, O., 2003. The sediment budget as conceptual framework and management tool.
922 Hydrobiologia 494, 71-82. doi: 10.1023/A:1025437509525

923 Smart, T., Hirst, D., Elston, D., 1999. Methods for estimating loads transported by rivers.
924 Hydrology and Earth System Sciences 3(2), 295-303. doi: 10.5194/hess-3-295-1999

925 Snoussi, M., Haïda, S., Imassi, S., 2001. Effects of the construction of dams on the water and
926 sediment fluxes of the Moulouya and the Sebou Rivers, Morocco. Regional Environmental
927 Changes 3(1), 5-12. doi: 10.1007/s10113-001-0035-7

928 Syvitski, J. P., Morehead, M. D., Bahr, D. B., Mulder, T., 2000. Estimating fluvial sediment
929 transport: The rating parameters. Water Resources Research 36(9), 2747-2760. doi:
930 10.1029/2000WR900133

931 Tanguy, J.M., 2013. Environmental Hydraulics: Modeling Software. Wiley-ISTE, 320 pp.

932 Tena, A., Batalla, R.J., Vericat, D., 2012. Reach-scale suspended sediment balance downstream
933 from dams in a large Mediterranean river. Hydrological Sciences Journal 57(5), 831-849. doi:
934 10.1080/02626667.2012.681784

935 Trimble, S.W., 2004. Effects of riparian vegetation on stream channel stability and sediment
936 budgets. In: Bennett, S.J., Simon, A. (Eds.), Riparian Vegetation and Fluvial Geomorphology.
937 American Geophysical Union, Washington, D.C., pp. 153-169. doi: 10.1029/008WSA12.

938 Turowsky, J.M., Rickenmann, D., Dadson, S.J., 2010. The partitioning of the total sediment
939 load of a river into suspended load and bedload: a review of empirical data. Sedimentology 57,
940 1126-1146. doi: 10.1111/j.1365-3091.2009.01140.x

941 U.S. Geological Survey, 2002. Determination of Channel-Morphology Characteristics, Bankfull
942 Discharge, and Various Design-Peak Discharges in Western Montana. Scientific Investigation
943 Report 2004-5263, 26 pp.

944 Vachtman, D., Sandler, A., Greenbaum, N., Herut, B., 2013. Dynamics of suspended sediment
945 delivery to the Eastern Mediterranean continental shelf. Hydrological Processes 27(7), 1105-
946 1116. doi: 10.1002/hyp.9265

947 Van Rompaey, A., Bazzoffi, P., Jones, R.J.A., Montanarella, L., 2005. Modeling sediment
948 yields in Italian catchments. Geomorphology 65, 157-169. doi:
949 10.1016/j.geomorph.2004.08.006

950 Vanmaercke, M., Poesen, J., Verstraeten, G., de Vente, J., Ocakoglu, F., 2011. Sediment yield
951 in Europe: Spatial patterns and scale dependency. Geomorphology 130, 142-161. doi:
952 10.1016/j.geomorph.2011.03.010

953 Vericat, D., Batalla, R.J., 2006. Sediment transport in a large impounded river: The lower Ebro,
954 NE Iberian Peninsula. Geomorphology 79, 72-92. doi: 10.1016/j.geomorph.2005.09.017

955 Vericat, D., Batalla, R.J., 2010. Sediment transport from continuous monitoring in a perennial
956 Mediterranean stream. Catena 82, 77-86. doi: 10.1016/j.catena.2010.05.003

957 Vericat, D., Batalla, R.J., Garcia, C., 2006. Transporte de fondo y dinámica sedimentaria en un
958 río altamente regulado: el bajo Ebro (NE Península Ibérica). Revista Brasileira de
959 Geomofologia 7(2), 39-49.

960 Vörösmarty, C.J., Meybeck, M., Fekete, B., Sharma, K., Green, P., Syvitski, J.P.M., 2003.
961 Anthropogenic sediment retention: major global impact from registered river impoundments.
962 Global and Planetary Change 39, 169-190. doi: 10.1016/S0921-8181(03)00023-7

963 Walling, D.E., 2008. The changing sediment loads of the world's rivers. In: Sediment Dynamics
964 in Changing Environments. Proceedings of the Christchurch Symposium, Christchurch, New
965 Zealand. IAHS Publication 325, 323-338. doi: 10.2478/v10060-008-0001-x

966 Walling, D.E., Webb, B.W., 1996. Erosion and sediment yield: a global overview. In: Erosion
967 and Sediment Yield: Global and Perspectives. Proceedings of the Exeter Symposium, UK.
968 IAHS Publication 236, 3-19.

969 White, W.R., Milli, W.R., Crabbe, A.D., 1975. Sediment transport theories: a review.
970 Proceedings of the Institution of Civil Engineers, London, Part 2, 59(2), pp 265-292.

971 Williams, G.P., Wolman, M.G., 1984. Downstream effects of dams on Alluvial Rivers. US
972 Geological Survey Professional Paper 1286, 83 pp.

973 Wolman, M.G., 1954. A method of sampling coarse bed material. American Geophysical Union
974 Transactions 35, 951-956. doi: 10.1029/TR035i006p0095

975 Wong, M., Parker, G., 2006. Reanalysis and Correction of Bed-Load Relation of Meyer-Peter
976 and Müller Using Their Own Database. Journal of Hydraulic Engineering 132(11), 1159-1168.
977 doi: 10.1061/(ASCE)0733-9429(2006)132:11(1159)

978 Yellow River Conservancy Commission, 2004. Artificial density flow - the new achievements
979 of the sediment transportation experiment on the Yellow River.

980 **Table 1**

981 Relations used to determine the suspended sediment concentrations (*SSC*) from turbidity data
982 and the suspended sediment load at the three sites for the study period [a]

983

Gauging station	mV-*SSC* relation			
	Rating curve	***n***	***R*²**	***p*-value**
EA050	$SSC = 0.374 \times Turb - 1.492$	148	0.872	<0.001
EA051	$SSC = 0.464 \times Turb - 1.259$	31	0.993	<0.001
EA012[b]	$SSC = 0.381 \times Turb - 2.038$	214	0.882	<0.001
	***Q*-*SSC* relation**			
	Rating curve		***R*²**	***p*-value**
EA050	$SSC = 1.885 \times Q + 3.451$		0.573	<0.001
EA051	$Q < 6$ m³ s⁻¹: $SSC = 19.269 \times Q$		0.758	<0.001
	$Q > 6$ m³ s⁻¹: $SSC = 1.852 \times Q + 110.76$		0.857	<0.001
EA012[b]	--		--	--

[a] *SSC* = suspended sediment concentration (mg l⁻¹); *Turb* = turbidity (mV); *Q* = discharge (m³ s⁻¹); *n* = number of samples used for calibration.

[b] Combined data from EA012, EA050, and EA051.

984 **Table 2**

985 Flow discharge and suspended sediment transport data for the study period at annual scale [a]

986

Gauging station / year	Flow discharge						Suspended sediment transport				
	Q_{mean} ($m^3 s^{-1}$)	*SD* ($m^3 s^{-1}$)	Q_{max} ($m^3 s^{-1}$)	Date Q_{max}	Q_{min} ($m^3 s^{-1}$)	Total runoff (hm^3)	SSC_{mean} ($mg l^{-1}$)	*SD* ($mg l^{-1}$)	SSC_{max} ($mg l^{-1}$)	Date SSC_{max}	Total *SSL* (t)
EA050											
2012-2013	1.3	9.4	353	06/03/2013	0.16	41.0	10.1	38.6	844	31/10/2012	5,492
2013-2014	0.54	1.4	24.7	29/09/2014	0.12	16.9	5.0	11.2	422	18/11/2013	424
2014-2015	0.99	5.4	164	29/11/2014	0.05	31.2	5.3	10.2	312	29/11/2014	1,918
EA051											
2012-2013	0.51	4.0	144	06/03/2013	0.08	16.1	7.4	21.8	911	21/10/2012	1,809
2013-2014	0.24	0.62	16.2	19/11/2013	0.09	7.6	4.5	9.4	141	19/11/2013	210
2014-2015	0.31	1.2	66.5	21/03/2015	0.06	9.8	5.5	11.9	234	21/03/2015	426
EA012											
2012-2013	1.3	1.6	41.3	06/03/2013	0.13	41.7	7.4	10.3	336	26/10/2012	390
2013-2014	0.76	0.90	0.45	14/06/2014	0.09	23.9	6.7	10.1	625	29/09/2014	171
2014-2015[b]	1.0	1.1	8.4	21/03/2015	0.18	31.6	-	-	-	-	-

[a] Q_{mean} = mean flow discharge; *SD* = standard deviation; Q_{max} = maximum flow discharge; Q_{min} = minimum flow discharge; *SSC* = suspended sediment concentration; SSC_{max} = maximum suspended sediment concentration; *SSL* = suspended sediment load. Statistics are based on hourly data.

[b] No data related to suspended sediment is available for 2014-15 at EA012.

Table 3

Flood analysis[a]: upstream from the dam only medium-large floods were considered (i.e., > 2 m^3 s^{-1}); downstream from the dam, floods were selected according to the upstream ones to facilitate comparison

Gauging station	Flood date	Duration[b] (h)	Max *Q* (m^3 s^{-1})	Runoff (hm^3)	Max *SSC* (mg l^{-1})	*SSL* (t)	*BL*[c] (t)	P[d] (mm)
EA050	21/10/2012	75	9.9	0.39	790	129	0.05	76.7
	31/10/2012	80	14.8	0.58	844	0.44	0.22	91.8
	06/03/2013[e]	138	353	17.4	599	512	4,846	339
	04/10/2013	88	3.2	0.41	40.0	4.3	0.03	47
	19/11/2013	138	24.7	3.4	422	274	23.1	199
	03/04/2014	114	16.8	1.6	239	85.0	0.94	86.6
	29/09/2014[f]	88	20.3	1.0	41.7	17.2	4.4	115
	29/11/2014[f]	189	164	11.2	312	1,412	2,340	323
	21/03/2015[f]	17	92.9	6.1	179	438	764	180
EA051	21/10/2012[e]	24	1.9	0.05	911	11.5		72
	31/10/2012[e]	27	2.7	0.09	154	2.2		79.5
	06/03/2013	109	144	7.2	364	1,715		188
	04/10/2013[f]	55	3.2	0.18	62.3	5.5		42.8
	19/11/2013[f]	84	16.2	1.3	141	129		164
	04/04/2014[f]	52	5.7	0.43	110	27.2		71.6
	29/09/2014[f]	65	11.7	0.45	132	25.7		110
	29/11/2014[f]	103	13.5	1.4	136	125		145
	21/03/2015[f]	37	66.5	1.5	234	229		132
EA012[g]	21/10/2012	6	2.5	0.02	275	2.8	-[h]	67.6
	31/10/2012	26	1.2	0.11	196	6.1	-	93.8
	06/03/2013	48	41.3	1.6	308	78.6	-	180
	18/11/2013	36	1.8	0.10	175	6.6	-	130
	03/04/2014	19	1.1	0.05	61.5	1.5	-	64.5
	29/09/2014[i]	22	3.0	0.09	625	17.1	-	146
	30/11/2014[i]	39	4.5	0.22	125	15.4	-	169
	21/03/2015	27	8.4	0.39	241	26.2	-	190

[a] *Max Q* = maximum discharge (m^3 s^{-1}); Max *SSC* = maximum suspended sediment concentration (mg l^{-1}); *SSL* = suspended sediment load (t); *BL* = bedload (t).

[b] Duration was considered to begin when *Q* was 1.5 times the base flow at the beginning of the flood (García-Ruiz et al., 2005), and ended at the second breakpoint of the recession curve converted to log values.

[c] Mean value of Bathurst (2007) and Recking (2010) formulae predictions.

[d] Precipitation was measured at the closest meteorological station.

[e] Hydrograph was estimated from another station.

[f] Suspended load was estimated from *Q*-*SSC* relations.

[g] No flood was observed at EA012 the 04/10/2013.

[h] Bedload was considered negligible.

[i] Flood episode with more than one peak. Floods were computed as one.

991 **Table 4**

992 Bedload data predicted for the study period at the annual scale

993

Gauging station / year	Bedload transport formulae		
	Bathurst (2007) (t)	Recking (2010) (t)	Mean (t)
EA050			
2012-2013	5,675	4,021	4,848
2013-2014	37.2	20.1	28.7
2014-2015	4,104	2,105	3104
Total	9,817	6,145	7,981
EA012			
2012-2013	- [a]	-	-
2013-2014	-	-	-
2014-2015	-	-	-
Total	-	-	-

	Estimation with regional values (t)
EA051	
2012-2013	1,807
2013-2014	1,459
2014-2015	1,549
Total	4,815

[a] Bedload is considered negligible.

994

995 **Table 5**

996 Sediment trapped in the reservoir according to the Heinemann method

997

Year	Suspension (t)	Bedload (t)	Total (t)
2012-2013	6,910	6,656	13,566
2013-2014	463	1,487	1,950
2014-2015	2,105	4,653	6,758
Total	9,478	12,796	22,274

998

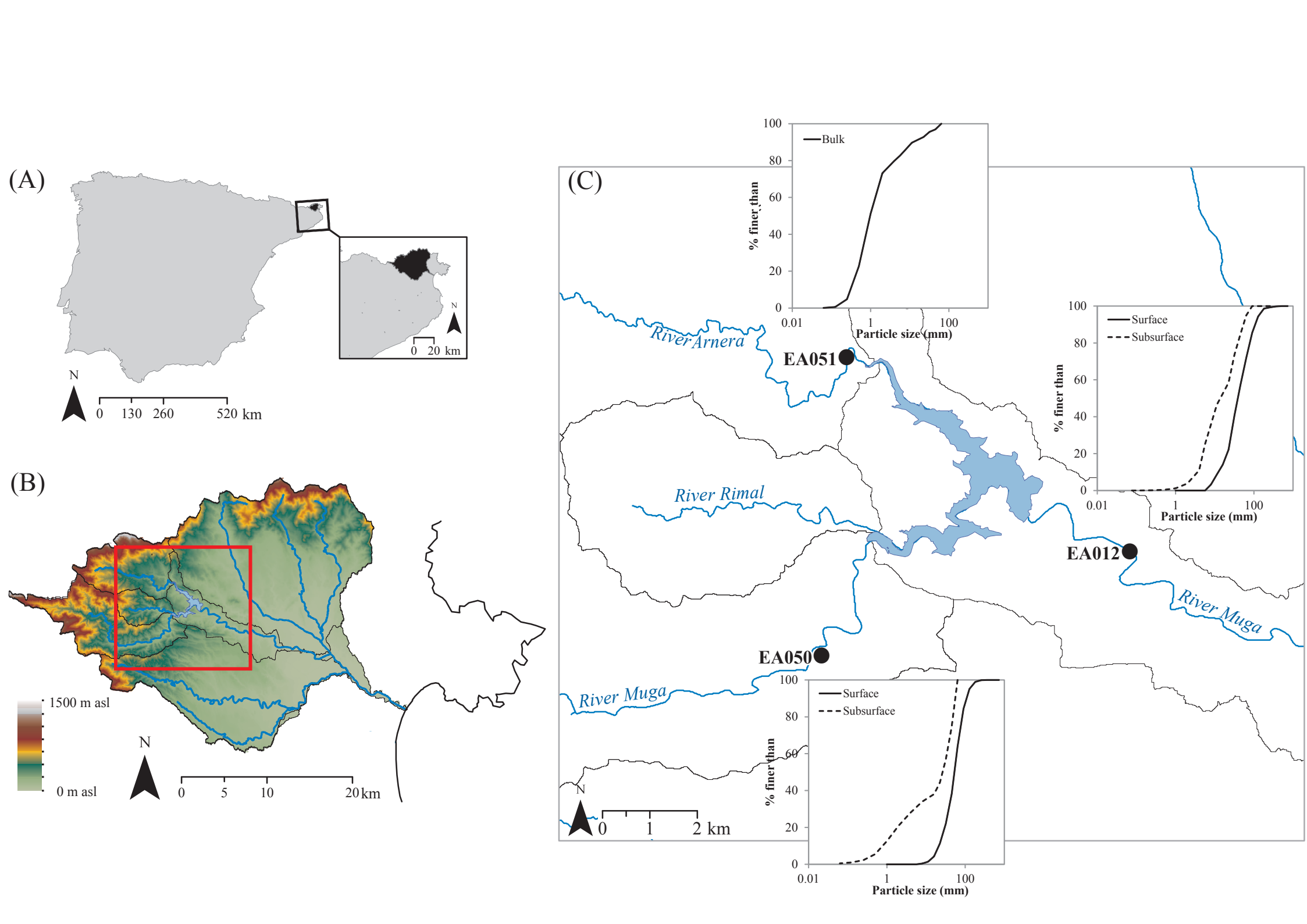
(A)
N
0 130 260 520 km
0 20 km
(B)
1500 m asl
0 m asl
N
0 5 10 20 km
(C)
River Arnera
River Rimal
River Muga
River Muga
EA051
EA012
EA050
N
0 1 2 km
Bulk
% finer than
Particle size (mm)
Surface
Subsurface
% finer than
Particle size (mm)
Surface
Subsurface
% finer than
Particle size (mm)

999 **Fig. 1.** (A) Location of the River Muga basin in the Iberian Peninsula; (B) altitudinal
1000 distribution of the Muga basin, with the main subbasins represented; (C) location of the study
1001 sites upstream and downstream from the Darnius-Boadella Reservoir. Grain size distribution
1002 graphs are shown for each site.

1003

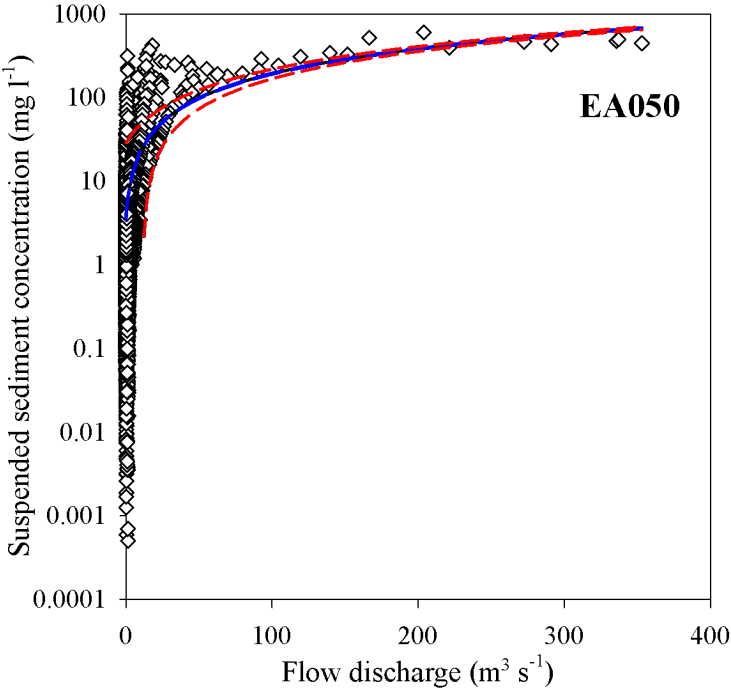
EA050
Suspended sediment concentration (mg l-1)
1000
100
10
1
0.1
0.01
0.001
0.0001
0
100
200
300
400
Flow discharge (m3 s-1)

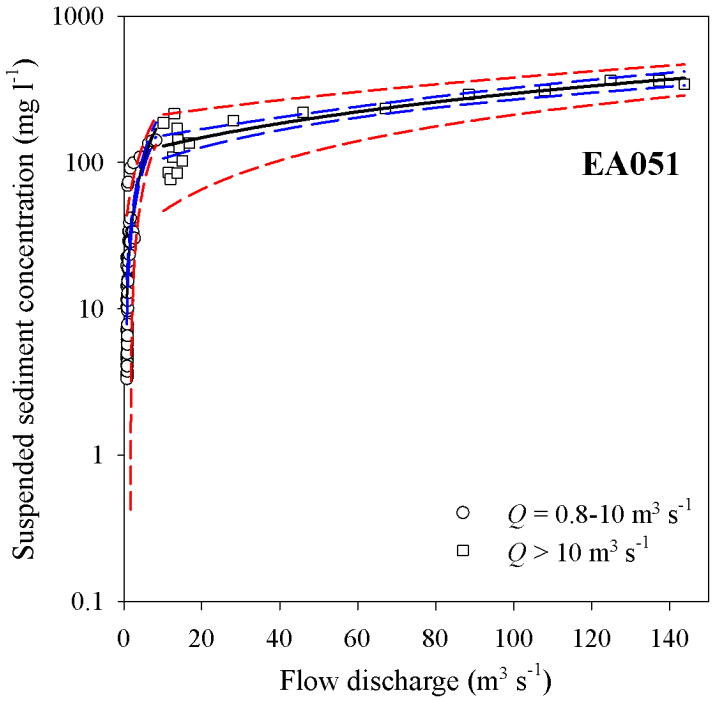
EA051
Suspended sediment concentration (mg l-1)
1000
100
10
1
0.1
Q = 0.8-10 m3 s-1
Q > 10 m3 s-1
0
20
40
60
80
100
120
140
Flow discharge (m3 s-1)

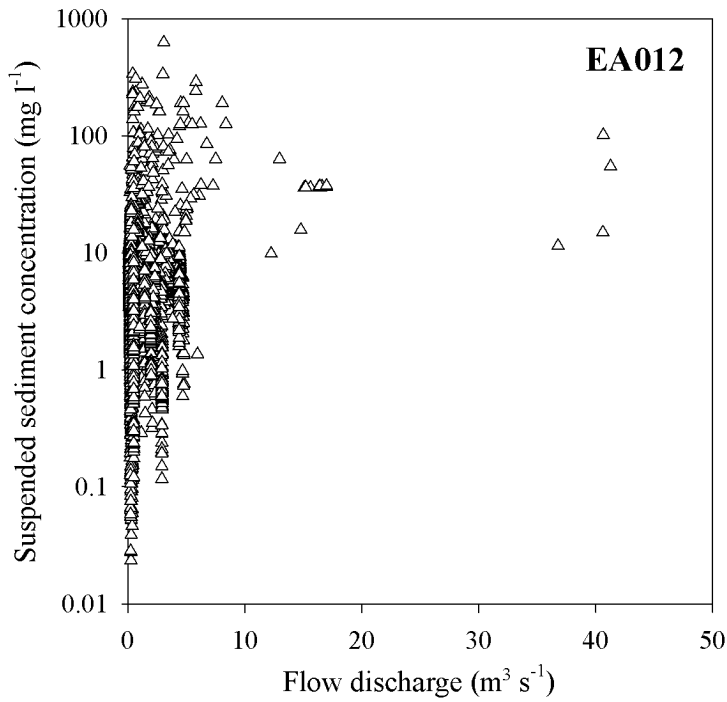
EA012
Suspended sediment concentration (mg l-1)
1000
100
10
1
0.1
0.01
0
10
20
30
40
50
Flow discharge (m3 s-1)

1004 **Fig. 2.** Suspended sediment load rating curves at the three monitoring stations. *SSC* data
1005 correspond to the available turbidity data. Blue dashed lines correspond to the 95% confidence
1006 bands, and red dashed lines correspond to the 95% prediction bands, above and below the
1007 regression line (in black), except for the EA012 site where no relationship was found. For
1008 clarity, the three sets of data are displayed in individual graphs, but note that the different scale
1009 ranges in both axes reflect the differences upstream and downstream from the dam. See Table 1
1010 for equations and statistical details.

1011

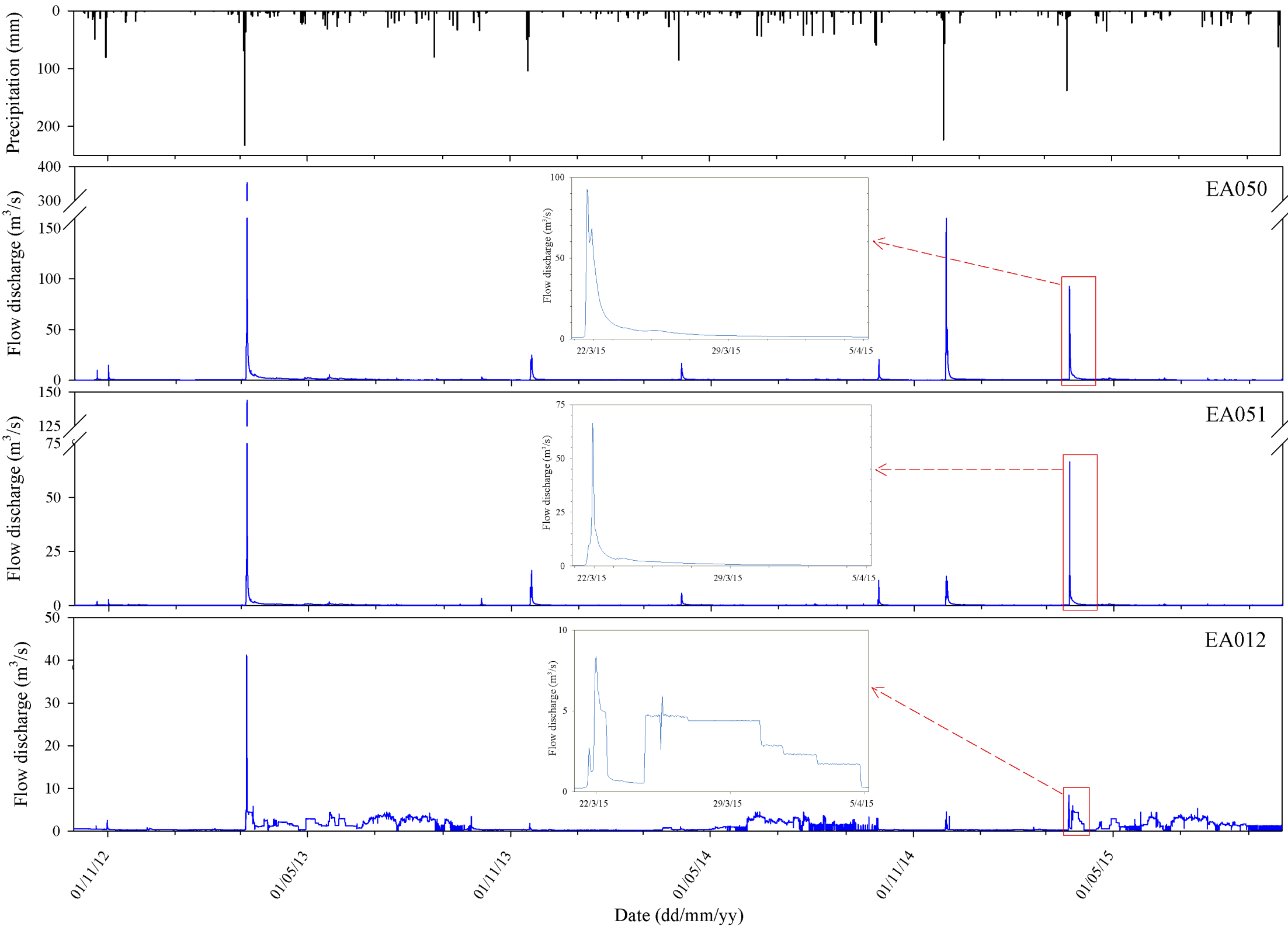
Precipitation (mm)
0
100
200
400
300
150
100
50
0
Flow discharge (m³/s)
EA050
100
50
0
Flow discharge (m³/s)
22/3/15
29/3/15
5/4/15
150
125
75
50
25
0
Flow discharge (m³/s)
EA051
75
50
25
0
Flow discharge (m³/s)
22/3/15
29/3/15
5/4/15
50
40
30
20
10
0
Flow discharge (m³/s)
EA012
10
5
0
Flow discharge (m³/s)
22/3/15
29/3/15
5/4/15
01/11/12
01/05/13
01/11/13
01/05/14
01/11/14
01/05/15
Date (dd/mm/yy)

1012 **Fig. 3.** Hydrographs for the study period at the three sampling sites. Inset graphs reproduce the
1013 shape of hydrographs for the 21 March 2015 flood. For clarity, the three sets of data are
1014 displayed in individual graphs, but note the breaks and the different scale ranges in the y-axis to
1015 better reflect the differences upstream and downstream from the dam. Precipitation data
1016 correspond to a meteorological station at $Muga_{up}$ subbasin.

1017

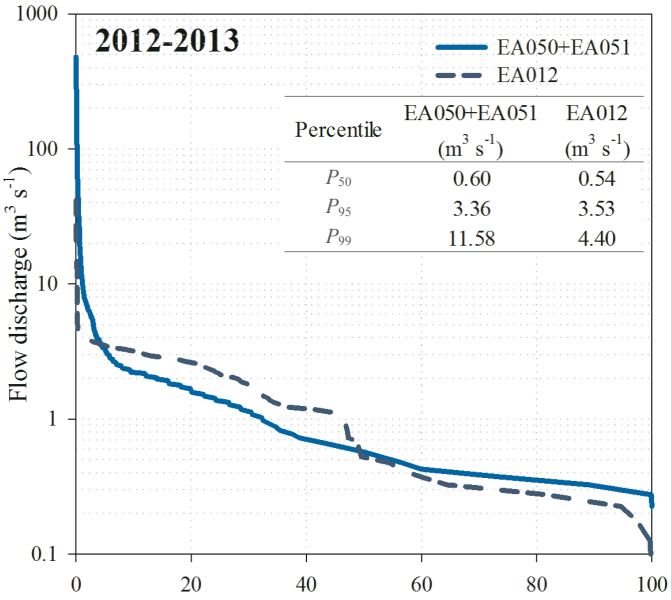
2012-2013
EA050+EA051
EA012
Percentile
EA050+EA051 (m3 s-1)
EA012 (m3 s-1)
P50 0.60 0.54
P95 3.36 3.53
P99 11.58 4.40
Flow discharge (m3 s-1)
1000
100
10
1
0.1
0
20
40
60
80
100

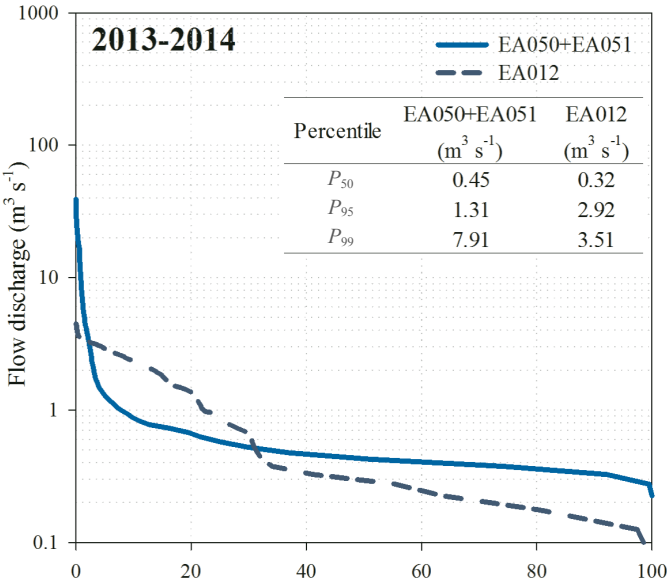
2013-2014
EA050+EA051
EA012
Percentile
EA050+EA051 (m3 s-1)
EA012 (m3 s-1)
P50 0.45 0.32
P95 1.31 2.92
P99 7.91 3.51
Flow discharge (m3 s-1)
1000
100
10
1
0.1
0
20
40
60
80
100

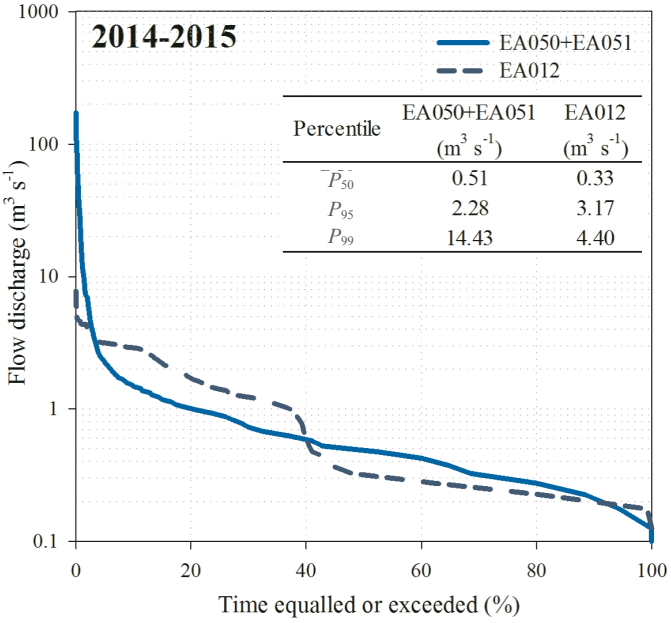
2014-2015
EA050+EA051
EA012
Percentile
EA050+EA051 (m3 s-1)
EA012 (m3 s-1)
P50 0.51 0.33
P95 2.28 3.17
P99 14.43 4.40
Flow discharge (m3 s-1)
1000
100
10
1
0.1
0
20
40
60
80
100
Time equalled or exceeded (%)

1018 **Fig. 4.** Flow duration curves calculated for the upstream (EA050+EA051) and the downstream
1019 (EA012) reservoir sections for individual hydrological years. The inset table shows the
1020 discharge associated to representative percentiles.

1021

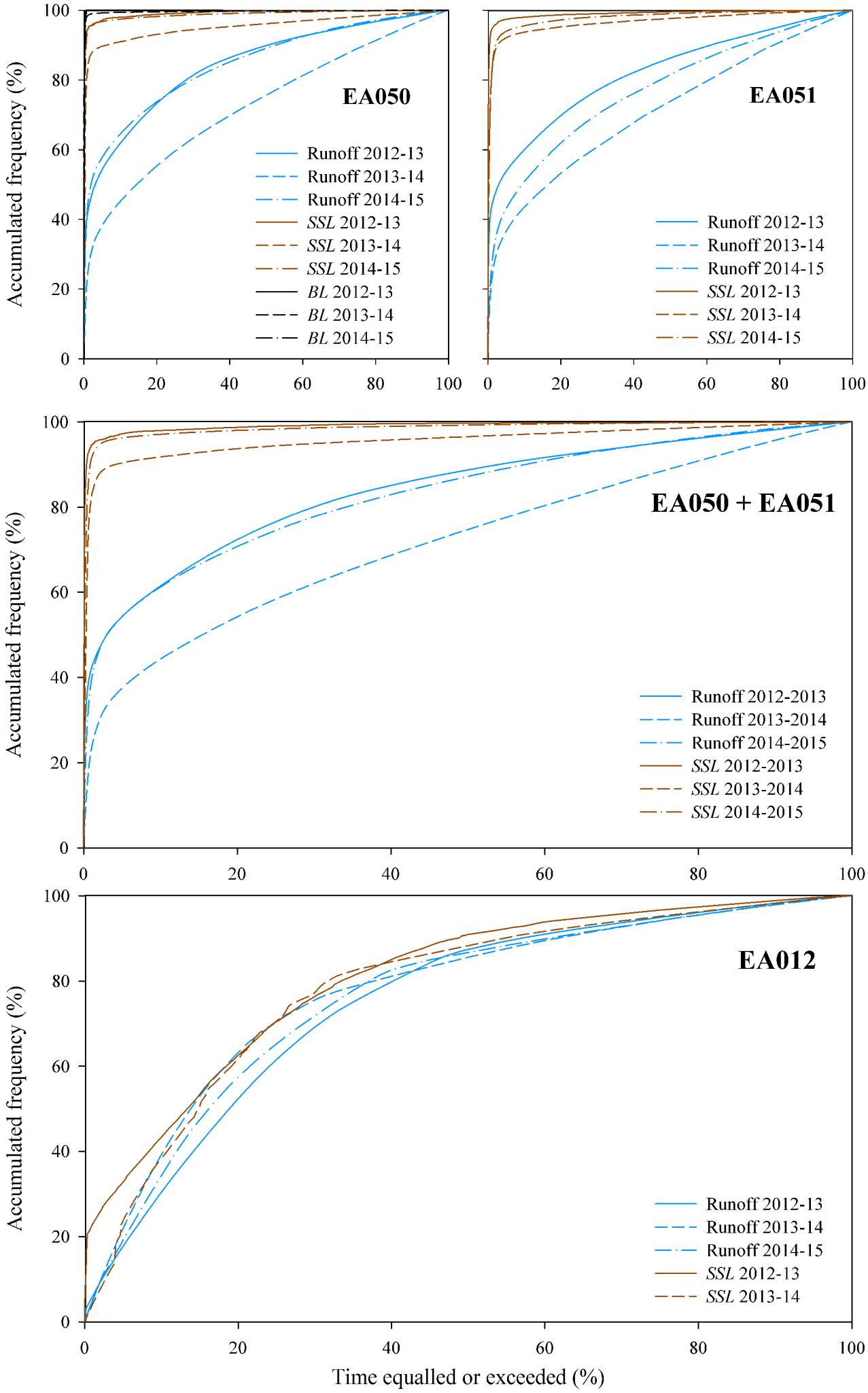
EA050
Runoff 2012-13
Runoff 2013-14
Runoff 2014-15
SSL 2012-13
SSL 2013-14
SSL 2014-15
BL 2012-13
BL 2013-14
BL 2014-15
EA051
Runoff 2012-13
Runoff 2013-14
Runoff 2014-15
SSL 2012-13
SSL 2013-14
SSL 2014-15
EA050 + EA051
Runoff 2012-2013
Runoff 2013-2014
Runoff 2014-2015
SSL 2012-2013
SSL 2013-2014
SSL 2014-2015
EA012
Runoff 2012-13
Runoff 2013-14
Runoff 2014-15
SSL 2012-13
SSL 2013-14
Accumulated frequency (%)
Time equalled or exceeded (%)
0
20
40
60
80
100

Fig. 5. Runoff and sediment load frequency curves of the monitoring sections for the three study years. Suspended sediment frequency curve for the year 2014-2015 at EA012 is not available because half of the year was estimated at the monthly scale. Bedload frequency curves are not available for the EA051 station as only a seasonal value was estimated. Bedload is considered negligible for the EA012 station, so curves are not drawn.

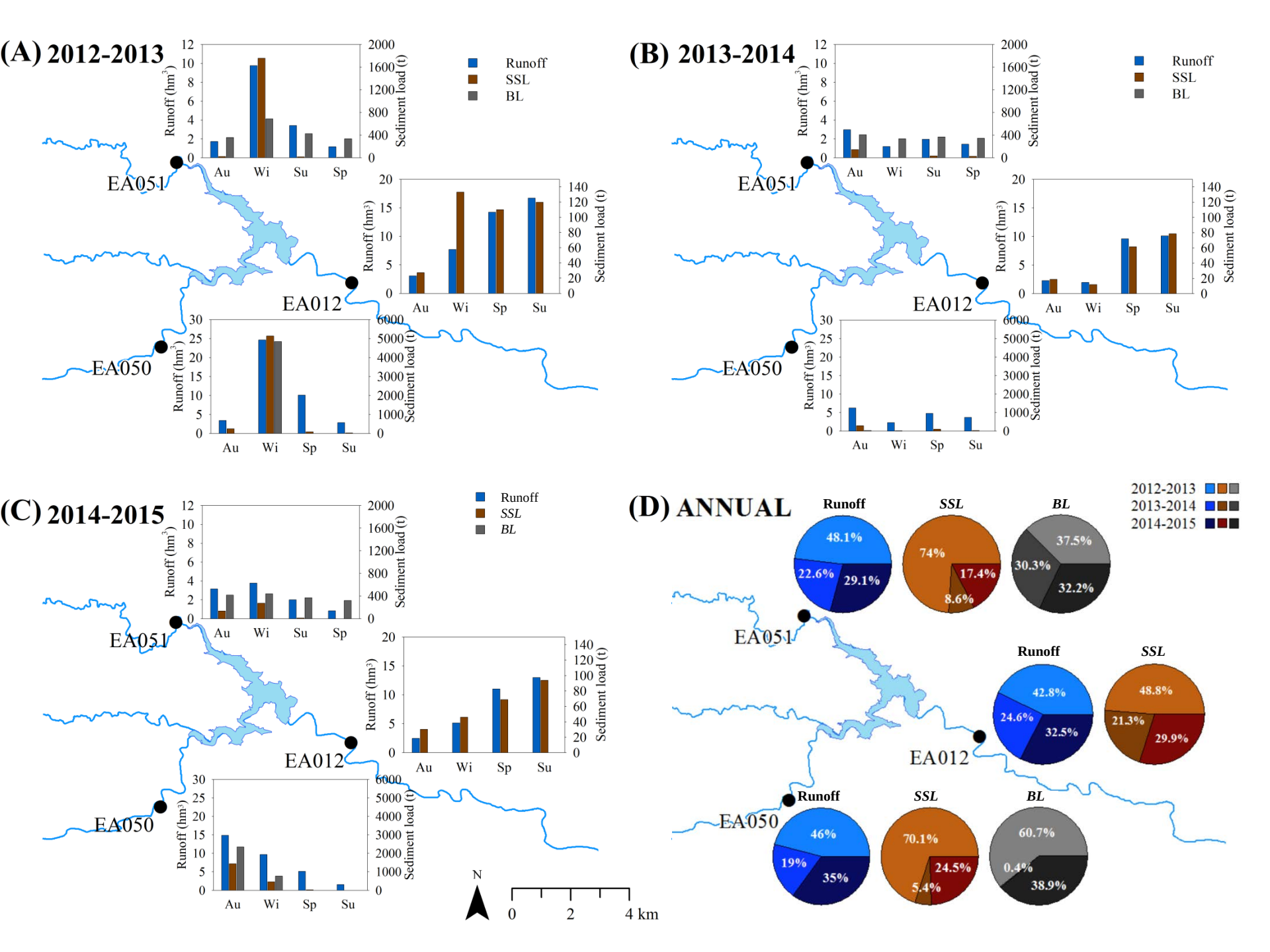
(A) 2012-2013
(B) 2013-2014
(C) 2014-2015
(D) ANNUAL
Runoff
SSL
BL
Runoff (hm³)
Sediment load (t)
Au
Wi
Su
Sp
EA051
EA012
EA050
2012-2013
2013-2014
2014-2015
48.1%
22.6%
29.1%
74%
17.4%
8.6%
37.5%
30.3%
32.2%
42.8%
24.6%
32.5%
48.8%
21.3%
29.9%
46%
19%
35%
70.1%
24.5%
5.4%
60.7%
0.4%
38.9%
N
0
2
4 km

1028 **Fig. 6.** Seasonal water and sediment budgets of the upper River Muga for (A) 2012-2013, (B)
1029 2013-2014, and (C) 2014-2015. (D) Annual distribution of water and sediment loads for the
1030 complete period 2012-2015. Seasons are established as Au (autumn): 1 Oct-31 Dec; Wi
1031 (winter): 1 Jan-31 Mar; Sp (spring): 1 Apr-30 Jun; Su (summer): 1 Jul-30 Sep.
1032